Tran-SET

Transportation Consortium of South-Central States

Solving Emerging Transportation Resiliency, Sustainability, and Economic Challenges through the Use of Innovative Materials and Construction Methods: From Research to Implementation

Durability of Concrete Produced with Alternative Supplementary Cementitious Material

Project No. 20CNMSU40

Lead University: New Mexico State University

Final Report

November 2021

Disclaimer

Acknowledgments

The authors would like to acknowledge the support and direction of the Project Review Committee that included Dr. Paul Barr of Utah State University, Ken Wylie of Wood Plc, and Sean Brady of the New Mexico Department of Transportation.

TECHNICAL DOCUMENTATION PAGE

1. **Project No.** 20CNMSU40	**2. Government Accession No.**	**3. Recipient's Catalog No.**

4. Title and Subtitle Durability of Concrete Produced with Alternative Supplementary Cementitious Material	**5. Report Date** Nov. 2021 **6. Performing Organization Code**
7. Author(s) PI: Craig M. Newtson https://orcid.org/0000-0002-2140-9759 Co-PI: Brad D. Weldon https://orcid.org/0000-0001-7196-8690 GRA: Judit M. Garcia https://orcid.org/0000-0002-9159-1525 GRA: Seyedsaleh Mousavinezhad https://orcid.org/ 0000-0003-0302-3796 GRA: William K. Toledo https://orcid.org/0000-0002-3436-5118	**8. Performing Organization Report No.**
9. Performing Organization Name and Address Transportation Consortium of South-Central States (Tran-SET) University Transportation Center for Region 6 3319 Patrick F. Taylor Hall, Louisiana State University Baton Rouge, LA 70803	**10. Work Unit No. (TRAIS)** **11. Contract or Grant No.** 69A3551747106
12. Sponsoring Agency Name and Address United States of America Department of Transportation Research and Innovative Technology Administration	**13. Type of Report and Period Covered** Project Proposal August 2020 – August 2021 **14. Sponsoring Agency Code**

15. Supplementary Notes

Report uploaded and accessible at: [Tran-SET's website (http://transet.lsu.edu/)](http://transet.lsu.edu/)

16. Abstract

Historically, Class F fly ash has been chosen as a supplementary cementitious material (SCM) in concrete for its ability to mitigate alkali-silica reaction (ASR). However, future availability of fly ash is uncertain because the energy industry has been investing in renewable energy production and removing coal burning generating stations from operation. Consequently, there is a growing need to find new, cost effective and environmentally friendly alternatives to fly ash. This study investigated a locally available natural pozzolan mined from a pumicite deposit near Espanola, NM for its ability to mediate ASR. Concrete and mortar mixtures included SCM contents ranging from 10 to 40%. Mortar bar tests and concrete tests for compressive and flexural strengths, shrinkage, frost resistance, chloride permeability, and surface resistivity were performed to assess the effectiveness of the pumicite. A minimum pumicite content of 20% was needed to mitigate ASR and that mortar mixtures containing 30% natural pozzolan had approximately 40% less expansion than mixtures containing 30% fly ash, indicating that the pumicite was substantially more effective at mitigating ASR than fly ash. Concrete mixtures containing natural pozzolan had comparable compressive strengths to specimens containing fly ash, while flexural strengths of specimens containing pumicite exceeded those of mixtures containing only fly ash. Concrete shrinkage decreased as pumicite content increased and when fly ash was used in place of pumicite. Fly ash mixtures produced at least 20% less shrinkage than similar 30% pumicite mixtures, indicating that the pumicite produced significantly greater shrinkage than the fly ash. Results also showed that mixtures containing 20 and 30% pumicite had the lowest acceptable durability factor (DF) values, and these DF values were significantly less than the DFs obtained using 30% fly ash. Rapid chloride permeability testing results showed that increasing pumicite content decreased chloride ion penetration. The 28-day surface resistivity results showed that the mixtures most susceptible to chloride ion penetration were the mixtures that contained either 10% natural pozzolan or 30% fly ash. Mixtures containing 30% fly ash provided substantially less chloride ion penetration resistance than mixtures containing 30% natural pozzolan at 28 days, but slightly better chloride resistance at 180 days. These results indicate that pumicite can reliably replace (partially or completely) fly ash for all of the durability issues addressed in this work.

17. Key Words Concrete, Natural Pozzolan, Alkali-Silica Reaction, Fly Ash, Durability	**18. Distribution Statement** No restrictions.

19. Security Classif. (of this report) Unclassified	**20. Security Classif. (of this page)** Unclassified	**21. No. of Pages** 49	**22. Price**

Form DOT F 1700.7 (8-72) **Reproduction of completed page authorized.**

SI* (MODERN METRIC) CONVERSION FACTORS

APPROXIMATE CONVERSIONS TO SI UNITS

Symbol	When You Know	Multiply By	To Find	Symbol
		LENGTH		
in	inches	25.4	millimeters	mm
ft	feet	0.305	meters	m
yd	yards	0.914	meters	m
mi	miles	1.61	kilometers	km
		AREA		
in^2	square inches	645.2	square millimeters	mm^2
ft^2	square feet	0.093	square meters	m^2
yd^2	square yard	0.836	square meters	m^2
ac	acres	0.405	hectares	ha
mi^2	square miles	2.59	square kilometers	km^2
		VOLUME		
fl oz	fluid ounces	29.57	milliliters	mL
gal	gallons	3.785	liters	L
ft^3	cubic feet	0.028	cubic meters	m^3
yd^3	cubic yards	0.765	cubic meters	m^3
		NOTE: volumes greater than 1000 L shall be shown in m^3		
		MASS		
oz	ounces	28.35	grams	g
lb	pounds	0.454	kilograms	kg
T	short tons (2000 lb)	0.907	megagrams (or "metric ton")	Mg (or "t")
		TEMPERATURE (exact degrees)		
°F	Fahrenheit	5 (F-32)/9 or (F-32)/1.8	Celsius	°C
		ILLUMINATION		
fc	foot-candles	10.76	lux	lx
fl	foot-Lamberts	3.426	candela/m^2	cd/m^2
		FORCE and PRESSURE or STRESS		
lbf	poundforce	4.45	newtons	N
lbf/in^2	poundforce per square inch	6.89	kilopascals	kPa

APPROXIMATE CONVERSIONS FROM SI UNITS

Symbol	When You Know	Multiply By	To Find	Symbol
		LENGTH		
mm	millimeters	0.039	inches	in
m	meters	3.28	feet	ft
m	meters	1.09	yards	yd
km	kilometers	0.621	miles	mi
		AREA		
mm^2	square millimeters	0.0016	square inches	in^2
m^2	square meters	10.764	square feet	ft^2
m^2	square meters	1.195	square yards	yd^2
ha	hectares	2.47	acres	ac
km^2	square kilometers	0.386	square miles	mi^2
		VOLUME		
mL	milliliters	0.034	fluid ounces	fl oz
L	liters	0.264	gallons	gal
m^3	cubic meters	35.314	cubic feet	ft^3
m^3	cubic meters	1.307	cubic yards	yd^3
		MASS		
g	grams	0.035	ounces	oz
kg	kilograms	2.202	pounds	lb
Mg (or "t")	megagrams (or "metric ton")	1.103	short tons (2000 lb)	T
		TEMPERATURE (exact degrees)		
°C	Celsius	1.8C+32	Fahrenheit	°F
		ILLUMINATION		
lx	lux	0.0929	foot-candles	fc
cd/m^2	candela/m^2	0.2919	foot-Lamberts	fl
		FORCE and PRESSURE or STRESS		
N	newtons	0.225	poundforce	lbf
kPa	kilopascals	0.145	poundforce per square inch	lbf/in^2

TABLE OF CONTENTS

LIST OF FIGURES

LIST OF TABLES

ACRONYMS, ABBREVIATIONS, AND SYMBOLS

ACRONYMS

AAR	Alkali-Aggregate Reaction
ACAA	American Coal Ash Association
AEA	Air-Entraining Admixture
ASR	Alkali-Silica Reaction
ASTM	American Society for Testing Materials
CHS	Calcium Silicate Hydrate
DF	Durability Factor
GGBFS	Ground-Granulated Blast Furnace Slag
HRWRA	High-range water-reducing admixture
MOR	Modulus of Rupture
NMDOT	New Mexico Department of Transportation
NMSU	New Mexico State University
RCPT	Rapid Chloride Permeability Testing
SCM	Supplementary cementitious material
Tran-SET	Transportation Consortium of South-Central States

ABBREVIATIONS

Al_2O_3	Aluminum Trioxide
BaO	Barium Oxide
$Ca(OH)_2$	Calcium Hydroxide
CaO	Calcium Oxide
Na_2O_e	Equivalent Sodium Oxide
OH^-	Hydroxyl Ions
Fe_2O_3	Iron Oxide
K^+	Potassium
MgO	Magnesium Oxide
MnO_2	Manganese Oxide
P_2O_5	Phosphorus Oxide

K_2O	Potassium Oxide
Si-OH	Silanol
SiO_2	Silica or Silicon Dioxide
Si-O-Si	Siloxane
$Si\text{-}O^-$	Silicon Monoxide
Na^+	Sodium
Na_2O	Sodium Oxide
SrO	Strontium Oxide
SO_3	Sulfur Trioxide
TiO_2	Titanium Dioxide

SYMBOLS

C	a constant that accounts for Poisson's ratio and the specimen's geometry
$CaO_{eq\alpha b}$	equivalent calcium oxide compound for a cementitious material
$CaO_{eq\alpha c}$	equivalent calcium oxide compound of a cement
$CaO_{eq\alpha fa}$	equivalent calcium oxide compound of fly ash
C_b	chemical ratio between CaO and SiO_2
E_0	the dynamic elastic modulus at zero cycles of freezing and thawing
E_{14c}	14-day accelerated mortar bar test expansion with cement only (no SCMs)
E_D	dynamic elastic modulus of a specimen
E_n	the dynamic elastic modulus after n cycles
m	the mass of the specimen
M	the specified number of cycles (300)
N	the number of cycles
$SiO_{2eq\beta b}$	equivalent silicon dioxide compound for a cementitious material
$SiO_{2eq\beta c}$	equivalent silicon dioxide compound of a cement
$SiO_{2eq\beta fa}$	equivalent silicon dioxide compound of fly ash
SR	surface resistivity measurement (kΩ-cm)
TCP	total charge passed during an RCPT (coulombs)

W	percent fly ash substitution by weight
ω_r	the measured fundamental frequency

EXECUTIVE SUMMARY

Alkali-silica reaction (ASR) is an expansive reaction that can occur between chemical components in cement and siliceous aggregates in concrete. The expansive nature of ASR causes internal tensile stresses that can lead to internal cracking that accelerates degradation. New Mexico, USA contains several of the most reactive siliceous aggregates in the world, making ASR the primary durability concern for concrete. Historically, supplementary cementitious materials (SCMs) such as Class F fly ash have been used to mediate ASR. The New Mexico Department of Transportation (NMDOT) requires that at least 20% Class F fly ash be used as a SCM in concrete mixtures to mediate ASR in an economical and sustainable manner. Unfortunately for the concrete industry, environmental considerations and changes in the energy industry are making Class F fly ash difficult to procure. Therefore, new cost effective and environmentally friendly alternatives to mitigate ASR must be identified and investigated.

This study is aimed at investigating the effects of using a locally available natural pozzolan mined from a pumicite deposit near Espanola, NM in concrete mixtures and its ability to mediate ASR. In this study, mortar bar testing was performed to identify cementitious material combinations capable of mediating ASR, which were then used to develop concrete mixtures that were characterized by assessing slump, air content, compressive strength, flexural strength, shrinkage, frost resistance, rapid chloride permeability, and surface resistivity. To evaluate the ability of the pumicite to replace fly ash in durable mixtures, concrete mixtures had pumicite contents ranging from 10 to 30% as well as total SCM contents that ranged from 10 to 40%.

A total of 22 mortar mixtures were produced and tested to investigate ASR mitigation. The mortar mixtures used pumicite to replace 10, 15, 20, 25, and 30% of the cement, fly ash to replace 30% of the cement, and combinations of fly ash and pumicite to replace up to 40% of cement. Control mixtures containing 100% cement were also produced. Each of these mixtures were produced using two aggregate sources, referred to as Placitas and Moriarty.

The ASR expansion results showed that increasing the natural pozzolan content reduced expansion and that a minimum pumicite content of 20% was needed to effectively mitigate ASR. Mortar mixtures containing 30% natural pozzolan had approximately 40% less expansion than mortar mixtures containing 30% fly ash, indicating that the natural pozzolan was substantially more effective at mitigating ASR than fly ash. Mortar mixtures that contained both pumicite and fly ash were the most effective for mitigating ASR.

Based on the results obtained for the ASR mortar bar tests, eight concrete mixtures were produced and tested using each aggregate source, for a total of 16 mixtures. Similar to the mortar bar mixtures, the concrete mixtures included mixtures that replaced 10, 20, and 30% of the cement with the natural pozzolan, replaced 30% of the cement with fly ash, and replaced up to 40% of cement with combinations of pumicite and fly ash.

Specimens containing 30% natural pozzolan had 7-day and 28-day compressive strengths that were comparable to strengths from specimens with 30% fly ash. In comparison, flexural specimens containing 30% pumicite exceeded the flexural strengths provided by mixtures containing only fly ash. This indicates that the natural pozzolan can be a desirable alternative for fly ash in terms of compressive and flexural strength. However, it was observed that

increasing the pumicite content decreased both the compressive strength and modulus of rupture of the concrete mixtures at 28-days.

Final shrinkage values for all of the concrete mixtures were less than 710 μstrain, which is below the 800 μstrain maximum limit used by many state departments of transportation. It was observed that shrinkage decreased as pumicite content increased and when fly ash was used in place of pumicite. It was also observed that mixtures with the greatest SCM contents (40%) experienced the least shrinkage. The 30% fly ash mixtures produced 21.1% and 31.7% less shrinkage than 30% pumicite mixtures for the Placitas and Moriarty aggregates, respectively, indicating that the pumicite produced significantly greater shrinkage than the fly ash.

Freezing and thawing tests showed that an adequate air void system was produced for each acceptable combination of cementitious materials. All concrete mixtures had durability factor (DF) values greater than 75, indicating that they were acceptable according to ASTM C666. The results also showed that mixtures containing 20 and 30% pumicite had the lowest DF values for both aggregate sources, and these DF values were significantly less than the DFs obtained using 30% fly ash. Increasing the total SCM content in concrete mixtures containing both fly ash and pumicite increased DF.

The 150-day rapid chloride permeability testing (RCPT) results showed that all concrete mixtures used in this study were categorized as having very low chloride ion penetration (less than 600 coulombs). Mixtures with 40% SCM had the greatest resistance to chloride ion penetration. The RCPT results also showed that increasing pumicite content from 10% to 30% decreased chloride ion penetration, indicating that pumicite was effective for preventing chloride ion ingress into concrete. Additionally, specimens containing 30% fly ash resulted in a lower charge passed than 30% natural pozzolan for both Placitas and Moriarty aggregates. However, the benefit of using fly ash was not substantial and should not cause any concern about replacing fly ash with pumicite.

Surface resistivity tests were performed at 28 and 180 days. Measured surface resistivity values at 180 days were much greater than 28-day surface resistivities. The 28-day surface resistivity results showed that the mixtures that were most susceptible to chloride ion penetration were the mixtures that contained either 10% natural pozzolan or 30% fly ash for both Placitas and Moriarty aggregates. Increasing pumicite content from 10% to 30% improved both 28-day and 180-day resistance to chloride ion penetration. Mixtures containing 30% fly ash provided substantially less chloride ion penetration resistance than mixtures containing 30% natural pozzolan at 28 days, but slightly better chloride resistance at 180 days. The 180-day surface resistivity measurements were reasonably consistent with the RCPT results when comparing their chloride ion penetration resistance categories and established correlation

1. INTRODUCTION

Alkali-silica reaction (ASR) is an expansive reaction that can occur between chemical components in cement and siliceous aggregates in concrete. The expansive nature of ASR causes internal tensile stresses that can lead to internal cracking. These cracks can drastically decrease the service life of concrete structures. New Mexico, USA contains several of the most reactive siliceous aggregates in the world. Consequently, ASR is the primary durability concern for concrete produced in New Mexico, USA.

Supplementary cementitious materials (SCMs) such as Class F fly ash have been commonly used in concrete to replace portland cement and mediate ASR. The New Mexico Department of Transportation (NMDOT) requires that at least 20% Class F fly ash be used as a SCM in concrete mixtures to mediate ASR. Class F fly ash is a reliable SCM for mediating ASR that also improves durability and mechanical properties of concrete, reduces materials costs, and improves sustainability (*1, 2*).

Class F fly ash is a byproduct formed during the combustion of coal to produce electricity. Unfortunately for the concrete industry, due to environmental considerations and changes in the energy industry, Class F fly ash is becoming difficult to procure. Therefore, new cost effective and environmentally friendly alternatives for mitigating ASR must be identified and investigated. A SCM that may have the potential to replace fly ash in durable concrete mixtures is a natural pozzolan that is being marketed as a SCM in New Mexico, USA.

This study is aimed at investigating the effects of using a locally available natural pozzolan mined from a pumicite deposit near Espanola, NM in concrete mixtures and its ability to mediate ASR. In this study, cementitious material combinations able to mediate ASR were identified from mortar bar tests. Concrete mixtures produced with acceptable cementitious material combinations were characterized by assessing slump, air content, compressive strength, flexural strength, shrinkage, frost resistance, rapid chloride permeability, and surface resistivity. To evaluate the ability of the pumicite to replace fly ash in durable mixtures, concrete mixtures had pumicite contents ranging from 10 to 30% as well as total SCM contents that ranged from 10 to 40%.

2. OBJECTIVES

The overall objective of this study was to assess the ability of a natural pozzolan to mediate ASR in mortar mixtures. The evaluation was performed by testing ASR mortar bar specimens containing a range of natural pozzolan contents, comparing their behavior with mortar mixtures that only contained fly ash, and also investigating a broad range of total SCMs contents for mixtures that contained combinations of fly ash and pumicite.

Once cementitious materials combinations were identified that would provide ASR durability, the next objective was to assess how the pumicite affected the mechanical and durability properties of concrete mixtures. Concrete mixtures were developed with a range of pumicite, fly ash, and SCM contents and were evaluated for strength and durability properties. Durability related tests that were conducted included shrinkage, frost resistance, rapid chloride permeability, and surface resistivity.

3. LITERATURE REVIEW

This chapter provides a literature review for concrete durability issues such as ASR, corrosion of reinforcing steel, and freezing and thawing, as well as a review of SCMs such as natural pozzolans that may affect concrete durability. Since the focal point of the durability issues addressed in this project was ASR, the ASR literature review includes details on the chemistry and mechanisms of ASR, factors that contribute to ASR and mitigation methods for ASR.

3.1. Alkali-Silica Reaction

Concrete is the most commonly used construction material in the world because it has versatile mechanical properties and has evolved to the point where it can provide good durability in nearly any environment. During the 1930s, Stanton (*3*) observed that some concrete structures developed cracks within a few years of their construction. Stanton (*3*) attributed the deterioration to alkali-aggregate reaction (AAR) and determined that the expansion of AAR was influenced by the amount and size of reactive silica, the amount of moisture present, and temperature. He also determined that the excessive expansions were controlled by the amount of alkali present in the cement and that expansion could be insignificant if the equivalent sodium oxide (Na_2O) content of the cement, Na_2O_e in Equation 1 was below 0.60%. Later studies focused on identifying the aggregate mineral components, assessing their reactivity, and identifying the mechanisms for their reaction (*4*).

$$Na_2O_e = Na_2O + 0.658K_2O \qquad [1]$$

3.1.1. Chemistry and Mechanisms of Alkali-Silica Reaction

ASR is an expansive chemical reaction that occurs between chemical compounds available in cement and certain siliceous rocks and minerals. The cement paste in concrete contains pores that allow water or ions in solution to migrate in what is known as the pore solution. The pore solution contains hydroxyl ions (OH^-) that react with silica (SiO_2) in certain aggregates to form a gel that is hydrophilic and swells in the presence of water (*5-7*). It is important to note that there are different forms of silica and that not all forms react significantly with the pore solution. Deleterious silica is composed of siloxane (Si-O-Si) or silanol (Si-OH) groups that react with high concentrations of OH^- and form negatively charged silicon monoxide ($Si\text{-}O^-$) ions (see Equations 2 and 3) (*5-7*). These negative charged $Si\text{-}O^-$ ions attract positively charged species such as sodium (Na^+) and potassium (K^+) available in the pore solution.

$$\text{Siloxane Groups: } Si\text{-}O\text{-}Si + 2OH^- \rightarrow 2Si\text{-}O^- + H2O \qquad [2]$$

$$\text{Silanol Groups: } Si\text{-}OH + OH^- \rightarrow Si\text{-}O^- + H_2O \qquad [3]$$

The Na^+ and potassium K^+ from the cement combine with the negatively charged $Si\text{-}O^-$ ions to form chemical reactions described in Equations 4 and 5 (*7*). The chemical composition of the alkali gel is indefinite, which adds complexity and variability to the chemical reactions that occur during ASR (*7*). The chemical reactions form a gel or silicate solution that expands by drawing moisture from the surrounding cement paste. The expansive properties of the gel are controlled by the amounts of alkali, reactive silica, and moisture that are present. Insignificant amounts of any of these components will result in negligible damage from ASR (*5-7*).

$$4SiO_2 + 2NaOH \rightarrow Na_2Si_4O_9 + H_2O \qquad [4]$$

$$3SiO_2 + 2NaOH \rightarrow Na_2Si_3O_7 + H_2O \qquad [5]$$

3.1.2. Silicates

Research has shown that not all siliceous aggregates are susceptible to ASR and that the reactivity of an aggregate is dependent on the mineralogy and crystalline structure of the aggregate. Poole (*4*) stated that aggregates are susceptible to ASR if they have one or more of the following characteristics: poor crystalline structures, multiple lattice defects, are microporous (large surface areas for reaction), are amorphous, or are glassy. Research has categorized minerals such as opal, certain forms of quartz, cristobalite, tridymite, chert, and volcanic glass as deleterious reactive minerals (*8*). Many of these minerals are found in several types of rocks but the reactivity of a certain aggregate source is dependent on the quantity of any particular mineral that the aggregate source contains.

Stanton (*3*) conducted a study on mortar bar specimens containing siliceous magnesian limestone with varying particle sizes, ranging from sub-180 µm to 6.7 mm. The specimens were grouped into four particle size categories (>180 µm, 180-600 µm, 0.6-2 mm, and 2-6.7mm) and by age (two, four, and six months). The results showed that a smaller particle size resulted in greater expansion for aggregate particles ranging from 180 µm to 600 µm. However, specimens containing particles smaller than 180 µm did not exhibit detrimental expansion. Stanton (*3*) hypothesized that the siliceous reactivity of the aggregate is reduced if not absent from a fine grained aggregate due to exhaustion of the reaction before it causes excessive expansive forces.

In a more recent study, Multon et al. (*10*) investigated the effects of aggregate size and alkali content on ASR. Six mortar mixtures that contained various amounts of reactive and non-reactive fine aggregates as well as different particle sizes for the fine aggregates were studied. Particle sizes were categorized into three size fractions: F1 (80–160 µm), F2 (315–630 µm), and F3 (1.25–3.15 mm). Additionally, the fine aggregates were characterized as reactive or non-reactive for each particle size category. The results showed that ASR expansion was seven times greater with coarser aggregate particles (F3) than with the finest ones (F1). Silica content was quantified for each particle size and showed that each size fraction contained approximately the same amount of reactive silica, so reactive silica content of the different fractions did not significantly influence the ASR results.

3.1.3. Importance of Equivalent Na_2O Content

Portland cement may contain some or all of the Na_2O and potassium oxide (K_2O) needed to react with silicates to produce ASR. However, Na_2O and K_2O can also be found in aggregates, SCMs, chemical admixtures, and external sources like seawater and deicing salts (*7*). Research has shown that ASR expansion increases with greater alkali concentrations. Stanton (*3*) determined that ASR was less likely to occur with cements containing less than 0.6% equivalent Na_2O content (Equation

1). Therefore, it was proposed to limit the alkali content in concrete by using cements with less than 0.6% equivalent Na_2O content. This constraint was implemented as an ASR prevention guideline for several decades until it was decided to limit the alkali content of the entire concrete mixture since Na_2O and K_2O could also be provided by admixtures or SCMs (*7*). Several studies have shown that limiting the alkali content of concrete to no more than 0.19 lb/ft^3 (3.0 kg/m^3) can effectively limit the effects of ASR.

3.1.4. Moisture

ASR cannot be activated without moisture. Moisture serves two distinct functions in the ASR expansion process. The first role is in the chemical reactions that lead to the formation of the expansive gel and the second role is the expansion of the gel resulting from sustained moisture that causes the physical damage in concrete (*10*). Consequently, deleterious ASR will not form in concretes that are dry in service since insufficient moisture in concrete will not cause the gel to expand (*6*). Specifically, research has shown that concretes with an internal relative humidity less than 80% will not experience expansive ASR (*12*). Studies have also shown that the internal relative humidity can be reduced by using a lower water-cement ratio (0.35 or less) and preventing external moisture from penetrating into the concrete (*7*).

3.1.5. Mitigation Methods

There are several methods that can be used to mitigate ASR including using non-reactive aggregates, limiting the alkali content in cement by using low-alkali cement, replacing a portion of the cement with SCMs, and using lithium compounds to inhibit the reaction (*5-7*). SCMs are one of the most reliable and economical mitigation methods. Utilizing SCMs as a partial replacement of portland cement is usually cost effective because many SCMs are waste products or naturally occurring materials. Additionally, many SCMs are environmentally friendly since they can be used to reduce portland cement production (*13*). It was noted by Farny and Kerkhoff (*6*) that restricting the use of non-reactive aggregates or using low-alkali cement is not always practical since non-reactive aggregates might not be economically viable and external alkali sources may limit the usefulness of low-alkali cements.

SCMs such as fly ash, slag, silica fume, and natural pozzolans have demonstrated effectiveness in mitigating ASR. Research has shown that combining multiple (two or three) cementitious materials can improve ASR mitigation. Fly ash and ground-granulated blast furnace slag (GGBFS) are the two most commonly used SCM’s. Unfortunately, fly ash is becoming more difficult to procure due to environmental considerations and changes in the energy industry. According to the American Coal Ash Association (ACAA) fly ash production has been decreasing for several years. In 2019, approximately 30 million tons of fly ash were produced, nearly a 50% drop in production compared to the 62.5 million tons that were produced in 2000 (*14*). The uncertain availability of Class F fly ash and the need to mitigate ASR in concrete requires that new cost effective and environmentally friendly alternatives be identified and investigated.

3.1.6. Chemical Index

Research has shown that fly ash is quite effective for mitigating ASR. The effectiveness of Class F fly ash is due to its chemical composition. Class F fly ash has been recognized as the most effective SCM due to its fineness, mineralogy, and chemical composition. Malvar and Lenke (*15*) conducted a study to determine the factors that make fly ash effective for mitigating ASR. The study also developed a chemical index to characterize the effectiveness of cement and fly ash combinations or determine the minimum amount of cement replacement that would be required to control expansion for various levels of aggregate reactivity. The chemical index can be calculated from the chemical composition of a fly ash using Equation 6:

$$C_b = \frac{CaO_{eq\alpha b}}{SiO_{2eq\beta b}} = \frac{CaO + 6.0\ (0.905Na_2O + 0.595K_2O + 1.39M_gO + 0.700SO_3}{SiO_2 + 1.0\ (0.589\ Al_2O_3 + 0.376Fe_2O_3)} \qquad [6]$$

where:

C_b = the chemical index for the chemical ratio between equivalent CaO and $SiO_{2;}$

$CaO_{eq\alpha b}$ = $\mathrm{CaO} + 6.0\ (0.905\mathrm{Na_2O} + 0.595\mathrm{K_2O} + 1.391\mathrm{MgO} + 0.700\mathrm{SO_3})$; and

$SiO_{2eq\beta b}$ = $\mathrm{SiO_2} + 1.0\ (0.589\mathrm{Al_2O_3} + 0.376\mathrm{Fe_2O_3})$.

The amount of fly ash needed to control expansion in a concrete mixture can be determined from Equation 7:

$$W = \frac{1 - 0.1778\ \tanh^{-1}\left(\frac{2 - \left(\frac{0.08}{E_{14c}}\right) - 1.0530}{1.0530}\right) + 0.7386}{\left(1 - \frac{CaO_{eq\alpha fa}}{CaO_{eq\alpha c}}\right) - \left(1 - \frac{SiO_{2eq\beta fa}}{SiO_{2eq\beta c}}\right)\left(0.1778\ \tanh^{-1}\left(\frac{2 - \left(\frac{0.08}{E_{14c}}\right) - 1.0530}{1.0530}\right) + 0.7386\right)} \qquad [7]$$

where:

W = the percent fly ash substitution by weight;

E_{14c} = 14-day accelerated mortar bar test expansion with cement only (no SCMs);

$CaO_{eq\alpha fa}$ = $\mathrm{CaO} + 6.0\ (0.905\mathrm{Na_2O} + 0.595\mathrm{K_2O} + 1.391\mathrm{MgO} + 0.700\mathrm{SO_3})$ (using the chemical composition of fly ash);

$CaO_{eq\alpha c}$ = $\mathrm{CaO} + 6.0\ (0.905\mathrm{Na_2O} + 0.595\mathrm{K_2O} + 1.391\mathrm{MgO} + 0.700\mathrm{SO_3})$ (using the chemical composition of portland cement);

$SiO_{2eq\beta fa}$ = $\mathrm{SiO_2} + 1.0\ (0.589\mathrm{Al_2O_3} + 0.376\mathrm{Fe_2O_3})$(using the chemical composition of fly ash); and

$SiO_{2eq\beta c}$ = $\mathrm{SiO_2} + 1.0\ (0.589\mathrm{Al_2O_3} + 0.376\mathrm{Fe_2O_3})$(using the chemical composition of portland cement).

Although Malvar and Lenke (*15*) focused on determining and maximizing the effectiveness of fly ash in concrete mixtures, their chemical index can also be used to assess the effectiveness of other SCMs.

3.2. Other Concrete Durability Issues

Other durability problems can also decrease the life expectancy of a concrete structure. Other durability properties addressed in this work include indicators of corrosion susceptibility for reinforcing steel such as rapid chloride permeability and surface resistivity, resistance to freezing and thawing, and shrinkage characteristics that may indicate susceptibility to cracking that would facilitate ingress of moisture and harmful chemical compounds.

3.2.1. Corrosion of Reinforcing Steel

Corrosion of reinforcing steel is the leading cause of deterioration in concrete structures. Corrosion is often initiated when harmful ions, such as chlorides, penetrate concrete and reach the reinforcing steel. Chloride ion penetration can occur through capillary absorption, hydrostatic pressure, diffusion, or evaporative transport (*16*). Corrosion of the steel creates ferrous oxide (rust) that occupies greater volume than the reactants. This expansion exerts internal tensile stresses in the concrete that can cause cracking in the surrounding concrete that can extend to the surface of the concrete and allow even more chloride ions to penetrate the concrete and accelerate the corrosion process. To protect reinforcing steel from corrosion, it is essential to limit chloride ion penetration into the concrete.

One way to improve resistance to chloride ion penetration is to use SCMs or other mineral admixtures to improve density by partially filling pore spaces. The SCMs produce secondary calcium silicate hydrate (CSH) that fills pore spaces to decrease pore volume and increases density. The pore volume in the cement paste largely controls the permeability of concrete and is affected by the cementitious materials used in the mixture and construction practices (*17*). Permeability can be assessed by conducting rapid chloride permeability testing (RCPT) or surface resistivity testing that determine electrical conductance and resistivity of the concrete mixture, respectively. Results from these tests provide indications of the ability of the concrete to resist penetration of chloride ions. In RCPT, greater electrical conductance in the concrete specimen indicates that the concrete is more permeable, while in surface resistivity testing, greater electrical resistivity indicates that a concrete specimen is less permeable (Table 1).

Table 1. RCPT and surface resistivity test interpretation.

Chloride Ion Penetrability	RCPT (total charge passed) (coulombs)	Surface Resistivity Test kΩ–in (kΩ-mm)
High	>4000	<4.7 (120)
Moderate	2000-4000	4.7-8.3 (120-210)
Low	1000-2000	8.3-14.6 (210-370)
Very Low	100-1000	14.6-100 (370-2540)
Negligible	<100	>100 (2540)

3.2.2. Freezing and Thawing

A cycle of freezing and thawing can cause degradation when the pore spaces in the concrete are filled (or nearly so) with water that will expand as it approaches its freezing temperature. When water freezes, it expands approximately 9%. As soon as the water expands, it causes internal pressures in the concrete. If the internal pressure exceeds the tensile strength of the concrete, it can cause the pore space to dilate and rupture *(18*). Microcracking near a pore can eventually lead to macrocracking, scaling, and severe degradation of the concrete after numerous cycles of freezing and thawing.

Research has shown that freezing and thawing effects can be mitigated by incorporating entrained air in the concrete. Air-entraining admixtures (AEAs) are usually used to improve frost resistance by creating air bubbles, ranging from 0.0004 to 0.04 in. (10 to 1000 μm) in diameter, in the cement paste that create space that can facilitate the expansion of ice in the concrete to prevent cracking (*19, 20*). Side effects that often occur when using AEAs include decreased strength and stiffness of the concrete (*19*). SCMs with high or variable carbon contents can jeopardize a concrete mixture's ability to entrain air and also make the air void system inconsistent across multiple batches of concrete (*21*).

Damage caused by freezing and thawing can be assessed by exciting vibration in specimens over a broad range of frequencies and recording the frequency with the greatest amplitude of acceleration. The frequency recorded is the resonant frequency for first mode vibration (fundamental frequency) and is related to the elastic modulus and density of the specimen (*22*). The fundamental frequency is used to determine the relative dynamic modulus, which can be monitored over multiple cycles of freezing and thawing to obtain an indication of the level of deterioration in a specimen.

3.2.3. Shrinkage

Shrinkage is the contraction of concrete volume due to the hydration reaction (chemical shrinkage), moisture loss to evaporation and hydration (drying shrinkage and self-desiccation), and decreasing temperature (thermal shrinkage). In this work, shrinkage is considered to occur in two stages: early-age shrinkage that occurs within the first 24 hours and long-term shrinkage that occurs after an age of 24 hours.

Early-age shrinkage consists of three phases: the liquid, skeletal structure, and hardening phases (*22*). The liquid phase commences as soon as the cementitious materials come into contact with water. During this phase, the concrete has no solid structure and cannot sustain stresses. Consequently, shrinkage in the liquid phase will only cause particles to shift and allow excess water to migrate to the surface. The second phase begins when cement hydration starts to form a skeletal structure (approximately initial set). The hardening phase occurs when the skeletal structure can sustain stresses. Long-term shrinkage can occur for several years and is dependent on several factors such as the chemical composition of the cementitious materials, amount of water in the original concrete mixture, surrounding environment, moisture conditions, and the size of the specimen.

Shrinkage can be assessed by measuring the change in size of a specimen. Typically, a specimen's length is monitored throughout its curing period and changes in length, relative to the initial length, quantify the amount of shrinkage that has occurred.

SCMs have been shown to decrease shrinkage by modifying the microstructure of the cement paste. Specifically, SCMs can help densify the concrete and create smaller pores in the matrix to reduce shrinkage (*24*). Research has shown that the ability of SCMs to reduce shrinkage is determined by the chemical composition of the SCM and the size and distribution of pores (*24*). In the case of fly ash, research has shown that increasing cement replacement by fly ash decreases both drying and autogenous shrinkage (25).

3.3. Supplementary Cementitious Materials

3.3.1. Common Supplementary Cementitious Materials

SCMs have been used to mitigate durability problems such as ASR, chloride penetration, freezing and thawing, and sulfate attack for many years. In many cases they have also been shown to improve mechanical properties of concrete. Fly ash, GGBFS, silica fume, and natural pozzolans are some of the most commonly used SCMs. Other SCMs, such as rice husk ash and metakaolin, have also been used to mitigate ASR. Additionally, Thomas et al. (*5*) highlighted studies where highly reactive recycled glass (crushed) and ground reactive silicate aggregates were used to mitigate the effects of ASR.

Fly ash is the most commonly used SCM in concrete and has been used since the 1930s. It is a byproduct of coal combustion produced from power plants. There are two classifications of fly ash, Class F and Class C fly ash, that are generally composed of varying amounts of calcium oxide (CaO), Na_2O, K_2O, magnesium oxide (MgO), sulfur trioxide (SO_3), SiO_2, aluminum trioxide (Al_2O_3), and iron oxide (Fe_2O_3) (*15, 26*). The chemical composition determines the ability of a fly ash to mitigate ASR. Studies have shown that while SiO_2, Al_2O_3, and Fe_2O_3 reduce expansion, CaO, Na_2O, K_2O, MgO, and SO_3 can increase expansion (*15*, 26). Class F fly ash is typically composed of expansion reducing compounds that make it more effective. For most reactive aggregates, 20% replacement of cement is generally adequate for controlling ASR expansion. Class C fly ash typically contains high levels of CaO and low amounts of SiO_2, making it less effective than Class F fly ash.

GGBFS has also been used for many years in concrete production. Slag is a byproduct of the iron industry and works like a pozzolan. Slag is typically composed of CaO, SiO_2, Al_2O_3, and MgO, along with some other minor oxides in small quantities. It has a glassy structure and produces CSH as a hydration product (*26*). When portland cement is hydrated it produces CSH and calcium hydroxide ($Ca(OH)_2$), the $Ca(OH)_2$ reacts with the slag and causes a chemical reaction that breaks down the chemical composition of the slag and separates it into a calcium rich phase and a silica rich phase. The phases then react with water to form CSH. A 50% cement replacement minimum is usually needed to effectively mitigate durability issues such as ASR (*26*). A higher cement replacement is needed, compared to fly ash, due to its chemical composition and specific chemical reactions. Slag is a slow reacting SCM that can require additional curing time and be susceptible to scaling.

Silica fume is a byproduct obtained from the production of silicon alloys. Silica fume consists primarily of fine (less than 0.00004 in. [1μm]) SiO_2 particles and is highly pozzolanic (*20*). The fineness of silica fume particles can cause an increase in water demand and require additional admixtures to maintain workability without increasing the water-to-cement ratio. Because of its fine particles, silica fume can increase the density of concrete as well as greatly improve strength and impermeability of concrete (*26*). Because silica fume greatly decreases concrete permeability, it is more effective for mitigating ASR than fly ash or slag. A minimum 10% cement replacement is usually needed to effectively mitigate ASR in concrete with highly reactive aggregates (*26*). Unfortunately, silica fume is substantially more expensive than other SCMs.

3.3.2. Pumicite and Other Natural Pozzolans

Natural pozzolans are a diverse class of siliceous or siliceous and aluminous materials that possess little or no cementitious ability when used by themselves, but are capable of reacting chemically with $Ca(OH)_2$ and water at normal temperatures to form compounds possessing cementitious properties that can greatly improve concrete durability and performance *(27-29*). Pumicite is amorphous and produced by the release of gases during the solidification of lava. Its cellular structure contains bubbles or air voids that result from gases being trapped in the molten lava during rapid cooling. Although these voids are elongated and parallel to one another, they are sometimes interconnected (*30*).

Research has shown that addition of pumicite powder to concrete reduces slump. Kabay et al. (*31*), observed that replacement of cement with pumicite powder, fly ash, and their blends produced concrete with lower water absorption, sorptivity, void contents, and lower early-age compressive and splitting tensile strengths.

Adding more, or coarser, pumicite to concrete may also reduce compressive strength and heat of hydration while increasing water demand and setting time as well as improving sulfate and ASR durability characteristics (*32, 33*). Liu et al. (*34*) reported that pumicite without stimulating additives, such as sodium silicate and potassium fluoride, had low pozzolanic activity.

Sarıdemir (*35*), reported that 25% pumicite addition to high strength concrete reduced 28-day compressive strength and modulus of elasticity. Other research has shown that 10% pumicite contributed significantly to microstructural density in high strength concrete, improved 180-day compressive and indirect tensile strengths, resistance to chloride ion penetration, and reduced 90-day water absorption (*36*).

In other research, mixtures containing fly ash, pumicite, or both had less 91-day compressive strength but more rapid strength development beyond 28 days than ordinary concrete (*37*). Additionally, self-compacting concrete produced with pumicite demonstrated good workability and achieved greater compressive strength at 120 days compared to mixtures without pumicite *(38*).

Pumicite has also been shown to produce acceptable resistance to freezing and thawing when used to replace up to 20% of the cement in concrete mixtures. However, 30% Pumicite decreased frost resistance significantly, as measured by durability factor (DF) (*39).*

4. METHODOLOGY

The following sections describe all of the materials used in this study as well as the methods used for ASR testing, concrete mixing, workability measurements, compression and flexural tests, shrinkage testing, frost resistance testing, RCPT, and surface resistivity testing.

4.1. Aggregates and Cementitious Materials

The materials used in this research were obtained locally in New Mexico, United States. The coarse aggregate, pea gravel, and sand were collected from two aggregate sources, the Placitas quarry near Bernalillo, New Mexico, USA and another quarry at Moriarty, New Mexico, USA. These aggregates are siliceous and are known to be extremely susceptible to ASR. The physical properties and particle size distributions of the aggregates are provided in Table 2 and Table 3, respectively. The cementitious materials used in this work included Type I/II low-alkali portland cement produced by GCC, class F fly ash produced at the San Juan generating station, and pumicite mined from a geological deposit. Chemical and physical properties of the cementitious materials are provided in Table 4.

Table 2. Aggregate physical properties.

Aggregate Source	Aggregate Type	Bulk Specific Gravity	Moisture Content (%)	Absorption (%)	Dry Rodded Unit Weight lb/ft^3 (kg/m^3)	Fineness Modulus
Placitas	Coarse Agg.	2.53	0.2	1.7	97.72 (1565)	-
	Pea Gravel	2.52	0.9	2.0	92.16 (1476)	-
	Sand	2.61	1.1	1.4	-	2.77
Moriarty	Coarse Agg.	2.65	0.2	1.7	98.11 (1572)	-
	Pea Gravel	2.66	0.2	1.3	95.54 (1530)	-
	Sand	2.70	0.9	1.2	-	3.40

Table 3. Particle size distribution (percent passing) of aggregates.

Aggregate Source	Aggregate Type	Sieve No.									
		3/4	1/2	3/8	4	8	16	30	50	100	PAN
Placitas	Coarse Agg.	62.8	8.9	5.7	7	6.8	1.1	-	-	-	0
	Pea Gravel	-	-	98.7	8.2	0.6	0.5	0.4	0.3	0.2	0
	Sand	-	-	-	98.4	84.7	70.9	49.9	16.8	2.9	0
Moriarty	Coarse Agg.	81.7	39.5	11.3	3.7	1.6	-	-	-	-	0
	Pea Gravel	-	-	93.2	7.5	3	1.9	1.8	1.3	1.1	0
	Sand	-	-	-	98.3	87.1	78.2	59.8	29.1	6.3	0

Table 4. Chemical and physical properties of cement, fly ash, and natural pozzolan (%mass).

Chemical Properties	Material		
	Cement Type I/II	Class F Fly Ash	Pumicite
SiO_2	20.3	53.16	76.29
Al_2O_3	4.6	24.64	12.13
Fe_2O_3	3.4	4.22	1.74
CaO	63.9	8.99	0.4
MgO	1.91	1.25	0.07
Na_2O	0.23	1.66	4.23
K_2O	0.38	1.24	4.29
TiO_2	-	-	0.1
MnO_2	-	-	0.08
P_2O_5	-	-	0.02
SrO	-	-	0.01
BaO	-	-	0.01
SO_3	2.86	0.25	0
Loss on Ignition	0.38	-	-
Physical Properties			
Specific Gravity	3.15	1.91	2.45
Spec. Surface Area ft^2/lb (m^2/kg)	1636 (335)	-	-
Autoclave Expansion (%)	0.05	0.01	-

4.2. Other Materials

To achieve the targeted workability of the concrete mixtures, commercially available chemical admixtures that included a high-range water-reducing admixture (HRWRA) and an AEA were added during mixing. The HRWRA that was used in this work was MasterGlenium 7920 and the AEA that was used was MasterAir AE-90.

4.3. Alkali-Silica Reaction Testing

Three mortar bar specimens were produced from each mortar mixture. Proportions for the mortar mixtures, which were produced with both aggregate sources using the same proportions, are presented in

Table 5. To interpret the names of the mortar mixtures, the first letter denotes the aggregate source, the following one, two, or three letter series denotes the cementitious materials used in the mixture, and the numbers after the second hyphen denote the cementitious materials contents (percent by mass) for each cementitious material in the mixture. For example, P-CNF-60/20/20 identifies the mixture with Placitas sand and cementitious materials that were comprised of 60% portland cement, 20% natural pozzolan, and 20% fly ash, by mass.

Table 5. Mortar mixture proportions.

Mixtures	Cement lb (g)	Pumicite lb. (g)	Fly ash lb. (g)	Fine Agg. lb (g)	Water lb (g)	HRWRA lb (g)
P-C-100	0.97 (440)	-	-	2.18 (990)	0.32 (145)	0.006 (2.87)
P-CN-90/10	0.58 (264)	0.39 (176)	-	2.18 (990)	0.32 (145)	0.006 (2.87)
P-CN-85/15	0.39 (176)	0.58 (264)	-	2.18 (990)	0.32 (145)	0.006 (2.87)
P-CN-80/20	0.19 (88)	0.78 (352)	-	2.18 (990)	0.32 (145)	0.006 (2.87)
P-CN-75/25	-	0.97 (440)	-	2.18 (990)	0.32 (145)	0.006 (2.87)
P-CN-70/30	-	0.97 (440)		2.18 (990)	0.32 (145)	0.006 (2.87)
P-CNF-75/10/15	0.29 (132)	0.58 (264)	0.097 (44)	2.18 (990)	0.32 (145)	0.006 (2.87)
P-CNF-75/15/10	0.44 (198)	0.39 (176)	0.15 (66)	2.18 (990)	0.32 (145)	0.006 (2.87)
P-CNF-67.5/22.5/10	-	0.87 (396)	0.097 (44)	2.18 (990)	0.32 (145)	0.006 (2.87)
P-CNF-60/20/20	-	0.78 (352)	0.19 (88)	2.18 (990)	0.32 (145)	0.006 (2.87)
P-CF-70/30	0.68 (308)	-	0.29 (132)	2.18 (990)	0.32 (145)	0.006 (2.87)
M-C-100	0.97 (440)	-	-	2.18 (990)	0.32 (145)	0.006 (2.87)
M-CN-90/10	0.58 (264)	0.39 (176)	-	2.18 (990)	0.32 (145)	0.006 (2.87)
M-CN-85/15	0.39 (176)	0.58 (264)	-	2.18 (990)	0.32 (145)	0.006 (2.87)
M-CN-80/20	0.19 (88)	0.78 (352)	-	2.18 (990)	0.32 (145)	0.006 (2.87)
M-CN-75/25	-	0.97 (440)	-	2.18 (990)	0.32 (145)	0.006 (2.87)
M-CN-70/30	-	0.97 (440)		2.18 (990)	0.32 (145)	0.006 (2.87)
M-CNF-75/10/15	0.29 (132)	0.58 (264)	0.097 (44)	2.18 (990)	0.32 (145)	0.006 (2.87)
M-CNF-75/15/10	0.44 (198)	0.39 (176)	0.15 (66)	2.18 (990)	0.32 (145)	0.006 (2.87)
M-CNF-67.5/22.5/10	-	0.87 (396)	0.097 (44)	2.18 (990)	0.32 (145)	0.006 (2.87)
M-CNF-60/20/20	-	0.78 (352)	0.19 (88)	2.18 (990)	0.32 (145)	0.006 (2.87)
M-CF-70/30	0.68 (308)	-	0.29 (132)	2.18 (990)	0.32 (145)	0.006 (2.87)

These mixtures were selected to investigate the effects that pumicite had on mitigating ASR expansion caused by two reactive fine aggregates. Specimen production, sampling, and testing procedures were performed according to ASTM C1567 (*40*). Prior to mixing, the two reactive fine aggregates were sieved and washed to meet the grading requirements from ASTM C1567 (*40*). Mortar bar specimens were cast in 1.0×1.0×11.25 in. (25.4×25.4×286 mm) steel molds with steel studs cast into each end of each mortar bar specimen. A water-to-cementitious materials ratio of 0.47 was used for each mixture. Additionally, a small amount, 0.006 lb. (2.87 g), of HRWRA was added to improve workability. To maintain the water-to-cementitious materials ratio of 0.47, the mixing water was reduced by the amount of water provided by the HRWRA. Mixing began by first adding the fine aggregates and cementitious materials into the mixer and dry mixing for 30 seconds. Then, two-thirds of the water was added to the mixer and mixing continued for another 30 seconds. Finally, the HRWRA was added and the remainder of the water were added to the mixer and mixed for three more minutes.

Initial length readings were taken for each mortar bar specimen prior to being immersed for a 24-hour period in a water bath that was raised to and then maintained at 176 ± 3ºF (80 ± 2ºC). A zero reading was taken after the 24-hour period to account for the thermal expansion the specimens experience. The specimens were then placed in a 1 N sodium hydroxide solution (NaOH) bath that was kept at 176 ± 3ºF (80 ± 2ºC) for 14 days. A length comparator was used to measure length changes of the specimens (Figure 1c) at one, three, five, seven, nine, 11, 13, and 14 days.

Measurements were taken within 15 seconds of a specimen being removed from the solution (Figure 1b). According to ASTM C1567 (*40*), mortar mixtures consisting of "combinations of cement, pozzolan, or GGBFS, and aggregate that expand more than 0.10% at 16 days after casting are indicative of potentially deleterious expansion" and are considered to be unacceptable mortar mixtures. However, some state transportation agencies use a more stringent expansion limit of 0.08%.

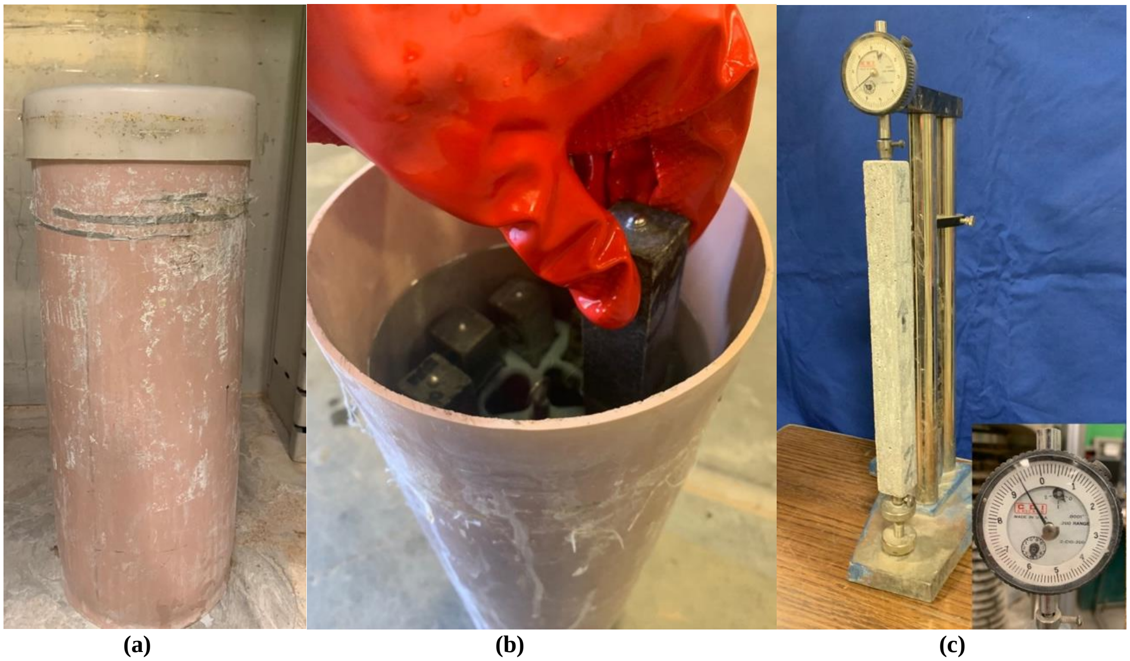
(a) **(b)** **(c)**

Figure 1. ASR Testing: (a) storage container, (b) removing sample from sodium hydroxide solution to take a reading, (c) dial gauge length comparator.

4.4. Mixture Proportions

This research investigated concrete mixtures produced using two aggregate sources. The series of concrete mixtures produced from each aggregate source consisted of eight concrete mixtures with a water-to-cementitious materials ratio of 0.35 and varying cement content, natural pozzolan content, fly ash content, HRWRA dosage, and AEA dosage. Proportions for 16 mixtures are presented in Table 6. For each mixture, the target slump and air content were 1.50 ± 1 in. (38.1 ± 25.4 mm) and 6.5% (-1 to +2%), respectively. In the mixture names, the first letter indicates the aggregate source, the letter N (for natural pozzolan) and a two-digit number indicating the natural pozzolan to cementitious materials ratio (%) appear after the first hyphen, and the letter F (for fly ash) and a two-digit number indicating the fly ash to cementitious materials ratio (%) appear after the second hyphen. For example, P-N22-F10 identifies the mixture with Placitas aggregates containing 22.5% pumicite and 10% fly ash as percentages of the total cementitious materials by mass.

Table 6. Concrete mixture proportions.

Mixture Name	Pumicite lb/yd^3 (kg/m^3)	Fly ash lb/yd^3 (kg/m^3)	Cement lb/yd^3 (kg/m^3)	Coarse Agg. lb/yd^3 (kg/m^3)	Pea Gravel lb/yd^3 (kg/m^3)	Sand lb/yd^3 (kg/m^3)	Water lb/yd^3 (kg/m^3)	HRWRA fl oz/yd^3 (mL/m^3)	AEA fl oz/yd^3 (mL/m^3)
P-N10-F00	73	-	656	1065	465	1244	256	32.8	29.2
	(43)		(389)	(632)	(276)	(738)	(152)	(1270)	(1130)
P-N20-F00	146	-	583	1065	465	1227	256	36.5	29.2
	(87)		(346)	(632)	(276)	(728)	(152)	(1410)	(1130)
P-N30-F00	219	-	510	1065	465	1209	256	38.3	29.2
	(130)		(303)	(632)	(276)	(717)	(152)	(1480)	(1130)
P-N00-F30	-	219	510	1065	465	1144	256	40.1	29.2
		(130)	(303)	(632)	(276)	(679)	(152)	(1550)	(1130)
P-N10-F15	73	109	547	1065	465	1185	256	40.1	29.2
	(43)	(64)	(325)	(632)	(276)	(703)	(152)	(1550)	(1130)
P-N15-F10	109	73	547	1065	465	1196	256	40.1	29.2
	(64)	(43)	(325)	(632)	(276)	(710)	(152)	(1550)	(1130)
P-N22-F10	164	73	492	1065	465	1183	256	40.1	29.2
	(97)	(43)	(292)	(632)	(276)	(702)	(152)	(1550)	(1130)
P-N20-F20	146	146	437	1065	465	1147	256	40.1	29.2
	(87)	(87)	(259)	(632)	(276)	(680)	(152)	(1550)	(1130)
M-N10-F00	73	-	656	1065	465	1364	256	32.8	29.2
	(43)		(389)	(632)	(276)	(809)	(152)	(1270)	(1130)
M-N20-F00	146	-	583	1065	465	1347	256	36.5	29.2
	(87)		(346)	(632)	(276)	(799)	(152)	(1410)	(1130)
M-N30-F00	219	-	510	1065	465	1329	256	38.3	29.2
	(130)		(303)	(632)	(276)	(788)	(152)	(1480)	(1130)
M-N00-F30	-	219	510	1065	465	1261	256	40.1	29.2
		(130)	(303)	(632)	(276)	(748)	(152)	(1550)	(1130)
M-N10-F15	73	109	547	1065	465	1303	256	40.1	29.2
	(43)	(64)	(325)	(632)	(276)	(773)	(152)	(1550)	(1130)
M-N15-F10	109	73	547	1065	465	1315	256	40.1	29.2
	(64)	(43)	(325)	(632)	(276)	(780)	(152)	(1550)	(1130)
M-N22-F10	164	73	492	1065	465	1300	256	43.7	29.2
	(97)	(43)	(292)	(632)	(276)	(771)	(152)	(1690)	(1130)
M-N20-F20	146	146	437	1065	465	1266	256	40.1	29.2
	(87)	(87)	(259)	(632)	(276)	(751)	(152)	(1550)	(1130)

To select proportions for mixtures containing Placitas aggregates, an existing concrete mixture approved by NMDOT was revised using the properties of Placitas aggregates measured in the lab. To proportion mixtures containing Moriarty aggregates, the masses of coarse aggregate and pea gravel were kept the same as the masses used for the Placitas mixtures. Since the Moriarty coarse aggregate and pea gravel had greater specific gravity and dry rodded unit weight than the Placitas coarse aggregate and pea gravel, the Moriarty mixtures contained slightly less coarse aggregate, volumetrically, than the Placitas mixtures. However, the fineness modulus of the Moriarty sand

(3.40) was significantly greater than that of the Placitas sand (2.77), so using even less Moriarty coarse aggregate could have been justified. However, the Moriarty coarse aggregate masses were not reduced since the resulting mixtures were not noticeably rockier than the Placitas mixtures, which was likely due to differences in the particle size distributions of the coarse aggregates from the two quarries.

4.5. Mixing

Mixing was performed in a 2 ft^3 (0.06 m^3) capacity drum mixer with an inclined rotation axis (Figure 2). The materials for each concrete batch were placed in the mixer, mixed, cast, and cured according to ASTM C192 (*41*). First, the coarse aggregates and a portion of the water (including the AEA) were added to the mixer and the mixer was started. After 30 seconds, the pea gravel, sand, cementitious materials, remaining water, and HRWRA were added with the mixer running. The concrete mixtures were mixed for three minutes and then allowed to rest for three minutes. Mixing was then continued for two additional minutes.

Immediately after mixing, slump and air content tests were conducted for each batch. For each mixture, twelve 4 by 8 in. (102 by 203 mm) cylinder specimens, two 6×6×24 in. (152×152×610 mm) beam specimens, and seven 3×4×16 in. (76×102×406 mm) prism specimens (four of which had gauge studs embedded in each end of the specimen) were cast. All specimens were demolded 24 hours after placement and cured according to ASTM C511 (*42*).

Figure 2. Concrete mixer.

4.6. Slump

Concrete workability was assessed by performing slump tests according to ASTM C143 (*43*). A steel slump cone that had a height of 12 in. (305 mm), a base diameter of 8 in. (203 mm), and a top diameter of 4 in. (102 mm) was used to perform the slump tests. The cone was placed on an even surface and filled in three equal (volumetrically) lifts with each lift rodded 25 times. The concrete was then struck off at the top of the cone to remove any excess concrete. The steel cone was then removed in a single motion by lifting it in the vertical direction. After inverting the steel cone and placing it next to the slumped concrete, the slump was immediately measured by placing a rod across the top of the inverted cone and measuring the slump from the top center of the concrete mound to the bottom of the rod as shown in Figure 3.

Figure 3. Slump test.

4.7. Air Content

Air content tests were performed according to ASTM C231 (*44*) using the pressure meter shown in Figure 4. To conduct the test, the base of the air meter was filled in three equal lifts, with each lift rodded 25 times. Excess concrete was struck off at the top of the container and the rim of the container was carefully cleaned to facilitate an airtight seal. The concrete air meter lid was then placed on top of the container and secured. Water was then poured into one of the valves until air stopped coming out of the other valve. The valves were then closed and the container was pressurized. The air content was measured and recorded within a few seconds of releasing pressurize air into the bottom container.

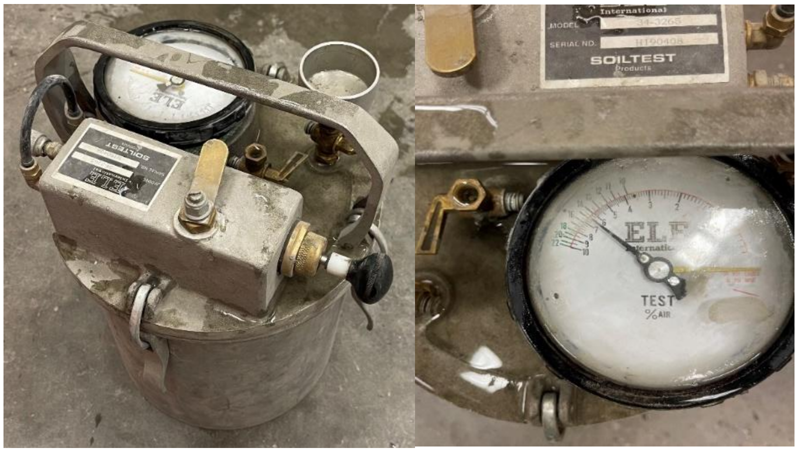

Figure 4. Air content test.

4.8. Compression Test

Compression tests were performed using a 400,000-lbf (2670 kN) capacity universal testing machine as illustrated in Figure 5. Compression tests were conducted according to ASTM C39 (*45*) using eight 4 by 8 in. (102 by 203 mm) cylinder specimens from each mixture, four were tested at an age of seven days and four were tested at an age of 28 days. During testing, neoprene caps were placed at both ends of the specimens (top and bottom ends) to distribute the load evenly to the specimen ends.

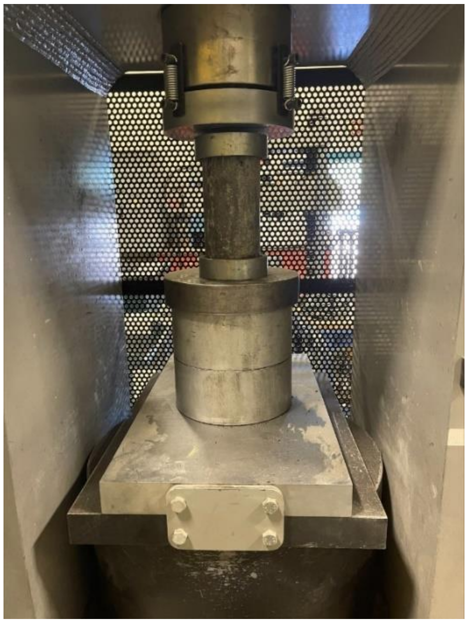

Figure 5. Compression test.

4.9. Flexural Test

To investigate 28-day flexural strength, two 6×6×24 in. (152×152×610 mm) beam specimens from each mixture were evaluated for modulus of rupture (MOR) according to ASTM C78 (*46*) as shown in Figure 6. Specimens were placed on two semi-circular end supports that were located 3 in. (76 mm) from each end of the beam and then loaded with two concentrated loads, spaced 6 in. (152 mm) apart, placed symmetrically about the midspan of the beam.

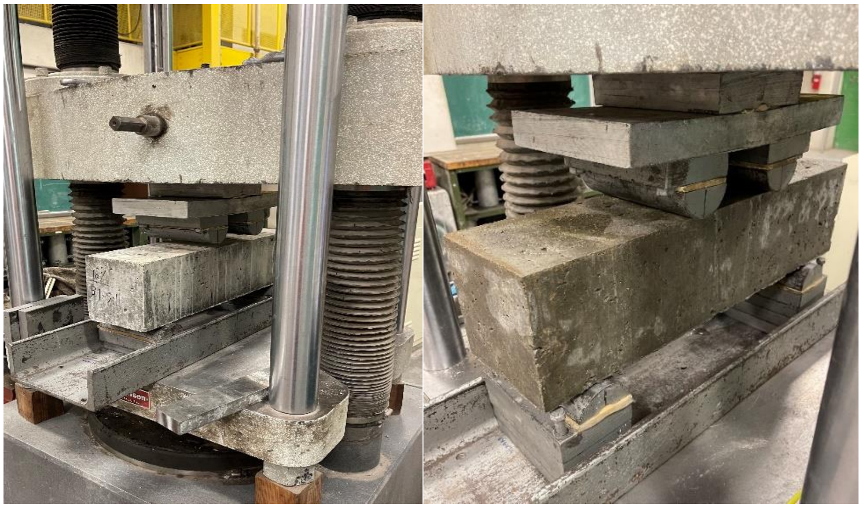

Figure 6. Flexural test.

4.10. Shrinkage

Shrinkage tests were performed to monitor length changes that the concrete mixtures experienced through wet curing and 28 days of drying after being removed from wet curing. These tests were performed according to ASTM C157 (*47*) on prismatic specimens that measured 3×4×16 in.

(76×102×406 mm). Specimens were allowed to cure for 23.5 ± 0.5 hours before they were removed from the steel molds and placed in a lime-saturated water maintained at 73 ± 3°F (23 ± 2 °C) for 30 minutes. Then, initial comparator readings were taken using the length comparator shown in Figure 7. Specimens were cured in lime-saturated water maintained at 73 ± 3°F (23 ± 2°C) for 28 days. After the 28-day curing period, the specimens were removed from the curing tank and the second length measurement was recorded. Specimens were then allowed to dry at ambient lab conditions, 69 ± 3°F (21 ± 2°C) and 30 ± 4% relative humidity. This relative humidity is drier than the 50% relative humidity stated in ASTM C157 (*47*), which leads to conservative shrinkage values (greater shrinkage). Length comparator readings were then recorded every three days for a 28-day drying period. Finally, average length changes for each mixture were used to compute shrinkage strain.

Figure 7. Shrinkage test.

4.11. Freezing and Thawing

Freezing and thawing tests, depicted in Figure 8, were performed on prismatic specimens according to ASTM C666 Procedure A (*48*). The prismatic specimens that measured 3×4×16 in. (76×102×406 mm) were experienced six to seven freezing and thawing cycles per day. Each specimen was subjected to a total of 300 freezing and thawing cycles. A full freezing and thawing cycle consisted of rapidly decreasing the temperature from 40 to 0°F (4.4 to -17.8°C) in approximately two hours and 20 minutes and increasing the temperature from 0 to 40°F (-17.8 to 4.4°C) in approximately one hour and 20 minutes The temperature was held constant at 0 °F (-17.8 °C) for eight minutes at the bottom of the temperature cycle. At the top of the temperature cycle, the temperature was held constant at 40°F (4.4°C) for 10 minutes. Mass and fundamental frequency measurements were taken at intervals that did not exceed 36 cycles. The mass and frequency data were used to calculate the dynamic elastic modulus of the specimens according to ASTM C215 (*49*).

The fundamental frequency measurements were performed according to the impact resonance method described in ASTM C215 (*49*). For the impact resonance method, an impact hammer is used to excite a wide range of frequencies in the specimen and the frequency at which the maximum amplitude occurs is recorded as the fundamental frequency. The fundamental frequency and the mass of the specimen are used to compute the dynamic elastic modulus of a specimen using Equation 8:

$$\mathrm{E_D = Cm\omega_r^2} \qquad [8]$$

where:
E_D = dynamic elastic modulus of a specimen;
C = a constant that accounts for Poisson’s ratio and the specimen’s geometry;
m = the mass of the specimen; and
ω_r = the measured fundamental frequency.

According to ASTM C215 (*49*), results from measurements obtained while monitoring deteriorating concrete should be presented in terms of the relative dynamic modulus (RDM) computed using Equation 9:

$$\mathrm{RDM = \frac{E_n}{E_o}(100)} \qquad [9]$$

where:
E_n = the dynamic elastic modulus after n cycles; and
E_0 = the dynamic elastic modulus at zero cycles of freezing and thawing.

After the freezing and thawing cycles were completed, Equation 10 was used to calculate the DF:

$$\mathrm{DF = \frac{RDM*N}{M}} \qquad [10]$$

where:
N = the number of cycles; and
M = the specified number of cycles (300).

Figure 8. Freezing and thawing test.

4.12. Rapid Chloride Permeability Test

RCPT was conducted to access the durability of concrete against chloride ion penetration (Figure 9). Specimen preparation and testing procedures were performed according to ASTM C1202 (*50*). RCPT was performed on 2-in. (51-mm) slices that were cut from 4 by 8 in. (102 by 203 mm) cylinder specimens at an age of 150 days. The specimens were then saw cut and allowed to dry for one hour before a rapid setting coating was brushed on the circumferential surface of the specimens. The slices were placed in a vacuum desiccator and the internal pressure was rapidly decreased to less than 0.965 psi (6650 Pa). Slices were kept in the vacuum desiccator for three hours before being submerged in deionized water for one hour with the pump running. The slices were kept in the vacuum desiccator for 18 hours while the pump was off. Then, the specimen slices were placed in the testing cells. The tests were performed using a power supply that was set to

60V DC and the current was measured every 30 minutes for six hours. The total charge passed (coulombs), that is a measure of the electrical conductance of the concrete during the period of the test, was calculated and plotted in accordance with ASTM C1202 (*50*).

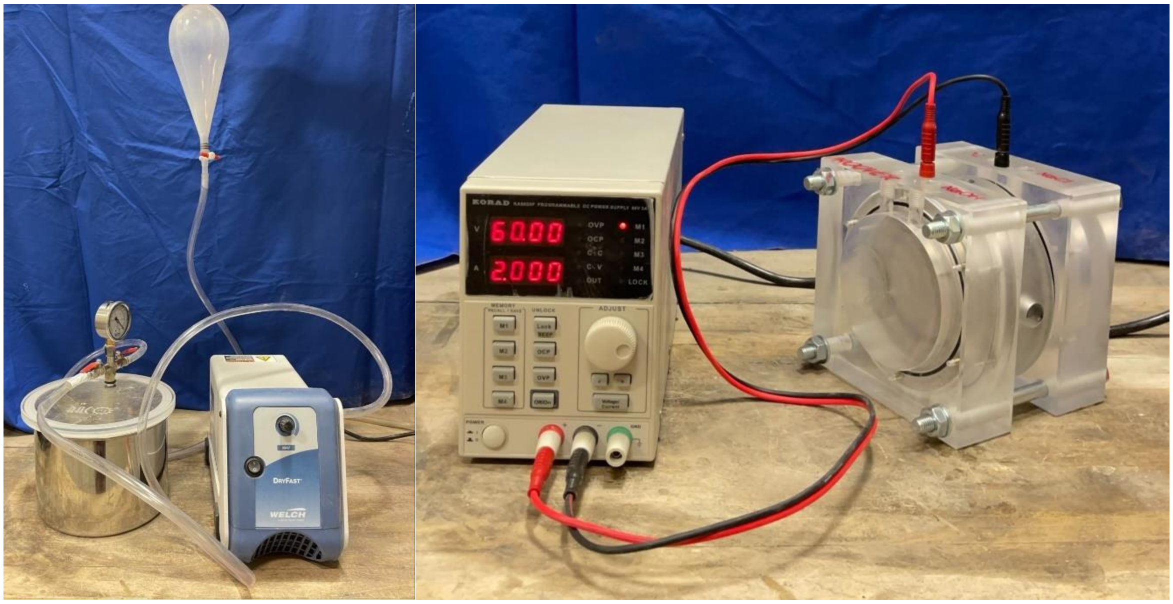

Figure 9. RCPT test.

4.13. Surface Resistivity

28-day and 180-day surface resistivity tests were performed to assess the ability of concrete to resist chloride ion penetration. Testing was conducted at 180 days for comparison with RCPT conducted at an age of 150 days. The surface resistivity test measures the electrical resistivity of specimens to provide a rapid indication of their resistance to chloride ion penetration. The equipment used to perform the surface resistivity tests was a Resipod Proceq, shown in Figure 10, that used a 4-Pin Wenner Probe Array. Testing was conducted on three cylinders from each mixture according to AASHTO T 358 (*51*).

Figure 10. Surface resistivity test equipment.

5. ANALYSIS AND FINDINGS

This chapter presents the results from the testing performed during this study. The tests that were conducted include ASR mortar bar tests, slump, air content, compression and flexural strength tests, shrinkage measurements, freezing and thawing tests, RCPT, and surface resistivity tests.

5.1. Alkali-Silica Reaction

Average ASR expansion results for all mortar mixtures are presented in Figures 11 and 12, and the final 14-day expansion values are provided in Table 7. Mortar specimens containing only low-alkali portland cement (P-C-100 and M-C-100) exhibited the greatest ASR expansions, with average expansions of 0.39% for the Placitas sand and 0.50% for the Moriarty sand. These expansion results exceed the ASTM C1567 (*40*) acceptable limit of 0.1% expansion and illustrate the extremely reactive nature of the two aggregate sources and that the Moriarty sand was more reactive than the Placitas sand.

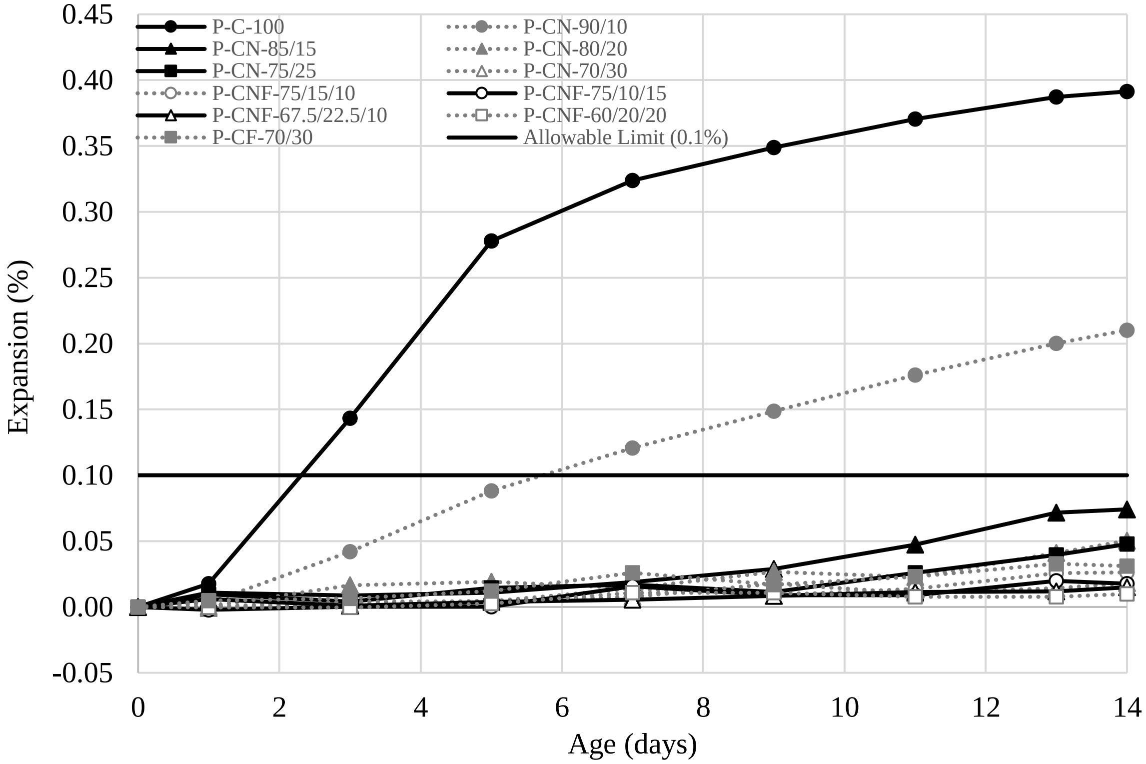

Figure 11. Placitas sand ASR results.

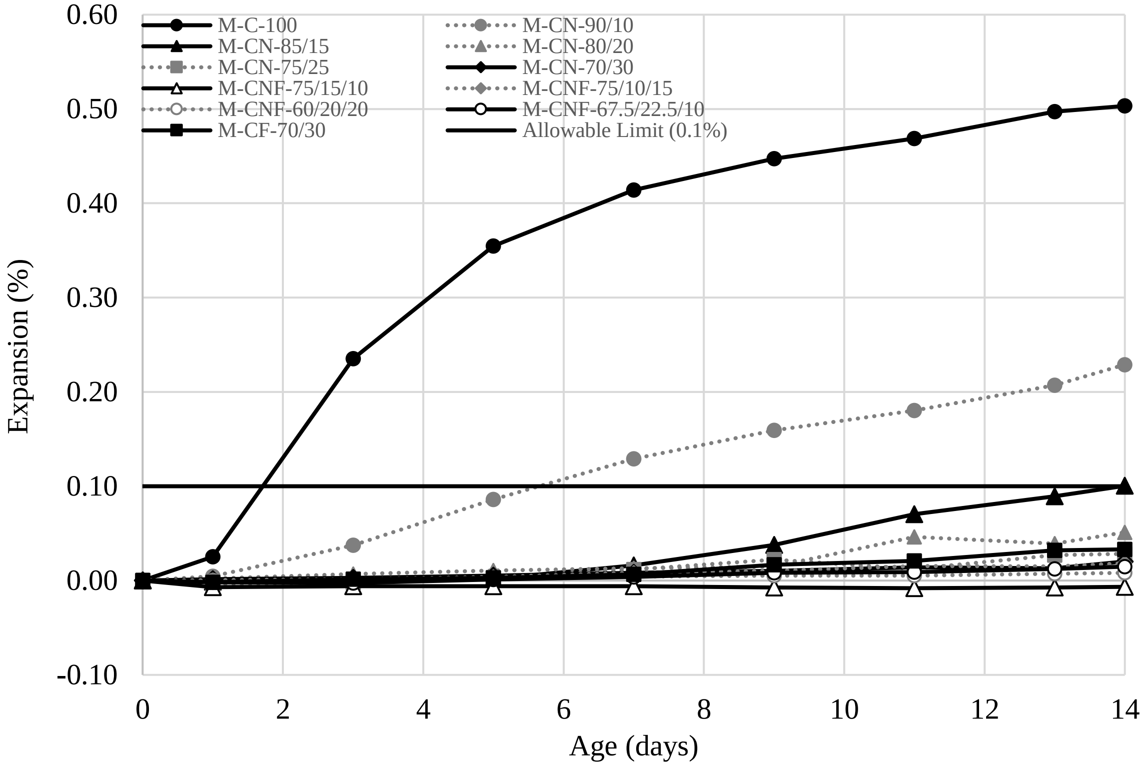

Figure 12. Moriarty sand ASR results.

Table 7. Average ASR expansion at 14 days.

Placitas Mixtures	Average Expansion (%) at 14-days	Moriarty Mixtures	Average Expansion (%) at 14-days
P-C-100	0.391	M-C-100	0.503
P-CN-90/10	0.210	M-CN-90/10	0.229
P-CN-85/15	0.074	M-CN-85/15	0.101
P-CN-80/20	0.050	M-CN-80/20	0.051
P-CN-75/25	0.048	M-CN-75/25	0.028
P-CN-70/30	0.018	M-CN-70/30	0.020
P-CNF-75/15/10	0.026	M-CNF-75/15/10	-0.007
P-CNF-75/10/15	0.018	M-CNF-75/10/15	0.018
P-CNF-67.5/22.5/10	0.015	P-CNF-67.5/22.5/10	0.015
P-CNF-60/20/20	0.010	M-CNF-60/20/20	0.008
P-CF-70/30	0.031	M-CF-70/30	0.033

Mortar mixtures P-C-100, P-CN-90/10, M-C-100, M-CN-90/10, and M-CN-85/15 had unacceptable expansion results that exceeded the ASTM C1567 limit (0.1%) (*40*). Consequently, mixtures that contained SCM contents of 15% or less were excluded from some of the other portions of this project.

The mortar mixtures presented in Table 8 are the mixtures that had acceptable ASR expansions according to the ASTM C1567 criteria (*40*). Most of these mixtures exhibited expansions that were less than 0.05%. Knowing that some state transportation agencies limit acceptable expansion to 0.08% does not change the acceptability of any of the mixtures listed in Table 8.

Table 8. Acceptable mortar mixtures according to ASTM C1567 (*40*).

Placitas Mixtures	Moriarty Mixtures
P-CN-85/15	-
P-CN-80/20	M-CN-80/20
P-CN-75/25	M-CN-75/25
P-CN-70/30	M-CN-70/30
P-CNF-75/15/10	M-CNF-75/15/10
P-CNF-75/10/15	M-CNF-75/10/15
P-CNF-67.5/22.5/10	P-CNF-67.5/22.5/10
P-CNF-60/20/20	M-CNF-60/20/20
P-CF-70/30	M-CF-70/30

Mortar mixtures P-CN-90/10, P-CN-85/15, P-CN-80/20, P-CN-75/25, P-CN-70/30, M-CN-90/10, M-CN-85/15, M-CN-80/20, M-CN-75/25, and M-CN-70/30 in Table 7 showed a strong trend where increasing natural pozzolan content improved the ability to mitigate ASR (reduced expansion). However, the pumicite was not able to control ASR expansion within acceptable limits for all mixtures since mixtures P-CN-90/10, M-CN-90/10, and M-CN-85/15 exhibited expansions greater than 0.1%. The excessive expansions for these mixtures indicate that a minimum natural pozzolan content of 20% is needed to effectively mitigate ASR.

Mortar mixtures P-CN-70/30 and M-CN-70/30 show that mixtures containing 30% natural pozzolan had less expansion, by approximately 40%, than mortar mixtures containing 30% fly ash (P-CF-70/30 and M-CF-70/30). This indicates that the pumicite was substantially more effective at mitigating ASR than fly ash.

Mortar mixtures that contained both natural pozzolan and fly ash were the most effective for mitigating ASR. Mixtures P-CNF-75/15/10, P-CNF-75/10/15, P-CNF-67.5/22.5/10, P-CNF-60/20/20, M-CNF-75/15/10, M-CNF-75/10/15, M-CNF-67.5/22.5/10, and M-CNF-60/20/20 all had expansions that were less than 0.03%. For the Placitas mixtures, increasing the SCM content improved the ability to mitigate ASR (reduced expansion) as expected. However, this trend was not evident for the Moriarty mortar mixtures. The lack of trend for the Moriarty mixtures seems to indicate that the variability of individual tests was greater than the strength of the trend. This is not unexpected since all of the Moriarty mixtures containing both fly ash and pumicite were essentially non-reactive, with expansions less than 0.02%.

The 25% natural pozzolan mixtures (P-CN-75/25 and M-CN-75/25) demonstrated that the pumicite was able to adequately control ASR expansion by itself. However, mixtures containing 15% natural pozzolan and 10% fly ash (P-CNF-75/15/10 and M-CNF-75/15/10) reduced expansions by at least 40% for both aggregate sources compared to P-CN-75/25 and M-CN-75/25, demonstrating the benefits of ternary mixtures. This observation can be used to facilitate a decrease in fly ash content from the 20% minimum fly ash content required by NMDOT to 10% for mixtures P-CNF-75/15/10 and M-CNF-75/15/10 when fly ash is available.

As stated in Chapter 3, Malvar and Lenke (*15*) conducted a study that developed a chemical index to characterize the effectiveness of cement and fly ash combinations or determine the minimum amount of cement replacement that would be required to control expansion for various levels of aggregate reactivity. Equation 7 was used to produce the plot shown in Figure 13 to estimate the amount of cement that should be replaced with pumicite to effectively mitigate ASR. The Placitas sand had a reference expansion (expansion of a reference mixture with no SCM) of 0.39%, while the Moriarty sand had a reference expansion of 0.50%. The plot in Figure 13 indicates that the minimum natural pozzolan contents, to replace equal masses of cement, were approximately 21% and 22% to mitigate the ASR expansion for the Placitas and Moriarty sands, respectively. The mortar bar tests performed during the current study showed that 20% and 15% pumicite contents were effective for mitigating ASR using Placitas and Moriarty sand, respectively. Based on this comparison, it appears that Malvar and Lenke's (*15*) model was conservative for the natural pozzolan.

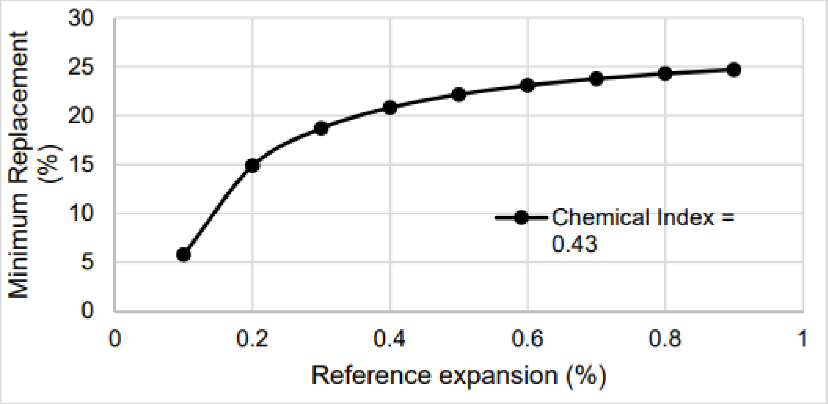

Figure 13. Estimated minimum pumicite replacement to mitigate ASR expansion as a function of reference expansion for specimens produced with only cement (no SCM).

5.2. Slump

Slump results from each concrete batch produced in this research are presented in Table 9. Each acceptable concrete mixture (presented in bold in Table 9) had an average of two slump measurements between 0.50 and 2.50 in. (12.7 and 63.5 mm), which is typically acceptable for a 1.50 in. (38.1 mm) target slump. In general, workability of mixtures produced with these admixtures and SCMs were consistent enough to achieve acceptable slumps in relatively few attempts. Specifically, no more than two adjustments to the HRWRA and AEA were needed to get slump within acceptable limits for any mixture, although there was one occurrence where slump alternated between acceptable and unacceptable values twice. Table 9 also shows that 27 trials were needed to produce 16 final mixtures with acceptable slumps and air contents. It should be noted that mixtures P-N10-F00 and P-N20-F00 were the first and the second mixtures produced in this research, respectively. When producing these mixtures, more trials were needed to meet specified ranges for slump and air contents due to lack of experience with the admixtures. After gaining experience with these two mixtures, it was much easier to meet the specified slump and air content ranges for the remaining mixtures.

It was observed that aggregate type did not seem to affect air content, but it did appear to influence slump. Comparing mixtures with different aggregate sources, but the same type and amount of cementitious materials (such as P-N30-F00 and M-N30-F00), shows that the amounts of HRWRA and AEA were constant but mixtures with Moriarty aggregates had less slump. This is most likely due, at least in part, to the Moriarty coarse aggregate contents being slightly greater than normal. The importance of this observation is minimal since the Moriarty mixtures were all acceptable in terms of workability, slump, compressive strength, flexural strength, and all of the durability related properties.

Table 9. Workability results.

Mixture Name	Trial No.	HRWRA fl oz/yd^3 (mL/m^3)	AEA fl oz/yd^3 (mL/m^3)	Slump in. (mm)	Air Content (%)
P-N10-F00	**Final**	**32.8 (1270)**	**29.2 (1130)**	**2.00 (50)**	**5.9**
	4th	32.8 (1270)	25.5 (990)	2.00 (50)	5.4
	3rd	36.5 (1410)	43.7 (1690)	2.25 (60)	9.8
	2nd	29.2 (1130)	43.7 (1690)	1.25 (30)	4.8
	1st	43.7 (1690)	29.2 (1130)	5.50 (140)	2.3
P-N20-F00	**Final**	**36.5 (1410)**	**29.2 (1130)**	**2.00 (50)**	**6.5**
	3rd	32.8 (1270)	43.7 (1690)	3.50 (90)	10.0
	2nd	32.8 (1270)	40.1 (1550)	1.75 (45)	4.7
	1st	36.5 (1410)	32.8 (1270)	3.00 (80)	5.1
P-N30-F00	**Final**	**38.3 (1480)**	**29.2 (1130)**	**2.50 (65)**	**7.3**
	1st	40.1 (1550)	29.2 (1130)	4.50 (115)	10.0
P-N00-F30	**Final**	**40.1 (1550)**	**29.2 (1130)**	**1.75 (45)**	**6.8**
	1st	38.3 (1480)	29.2 (1130)	0.25 (5)	6.0
P-N10-F15	**Final**	**40.1 (1550)**	**29.2 (1130)**	**2.25 (60)**	**6.6**
P-N15-F10	**Final**	**40.1 (1550)**	**29.2 (1130)**	**2.25 (60)**	**6.7**
P-N22-F10	**Final**	**40.1 (1550)**	**29.2 (1130)**	**2.00 (50)**	**6.6**
P-N20-F20	**Final**	**40.1 (1550)**	**29.2 (1130)**	**2.50 (65)**	**6.5**
M-N10-F00	**Final**	**32.8 (1270)**	**29.2 (1130)**	**1.75 (45)**	**5.8**
M-N20-F00	**Final**	**36.5 (1410)**	**29.2 (1130)**	**1.75 (45)**	**6.4**
M-N30-F00	**Final**	**38.3 (1480)**	**29.2 (1130)**	**2.00 (50)**	**7.3**
M-N00-F30	**Final**	**40.1 (1550)**	**29.2 (1130)**	**1.50 (40)**	**6.8**
	1st	38.3 (1480)	29.2 (1130)	1.00 (25)	4.5
M-N10-F15	**Final**	**40.1 (1550)**	**29.2 (1130)**	**1.75 (45)**	**6.6**
M-N15-F10	**Final**	**40.1 (1550)**	**29.2 (1130)**	**1.75 (45)**	**6.4**
M-N22-F10	**Final**	**43.7 (1690)**	**29.2 (1130)**	**1.75 (45)**	**6.5**
	1st	40.1 (1550)	29.2 (1130)	0.25 (5)	3.0
M-N20-F20	**Final**	**40.1 (1550)**	**29.2 (1130)**	**2.00 (50)**	**6.5**

5.3. Air Content

Table 9 also presents air content results for each concrete batch produced in this research. When considering the acceptable mixtures, the same AEA dosage was used to achieve the air content between 5.5% and 8.5% for all mixtures, even though the type of aggregates and type and amount of SCMs were varied. From this observation, it appears that air content was not particularly sensitive to aggregate source or SCM type. When aggregate source or the SCMs changed, air content changed, but not enough to push the air content out of the acceptable range.

It was expected that air content would be primarily influenced by AEA dosage. However, Table 9 shows that air content was usually adjusted by changing the HRWRA dosage. For example, the 2nd and 3rd trials of mixture P-N10-F00 show that increasing the HRWRA dosage and keeping the AEA dosage constant increased the air content. It appears that increasing the HRWRA dosage increased the fluidity of the fresh mixture and allowed the AEA to be more readily dispersed and activated than in a mixture with less workability. Additional evidence of this observation is provided by the fact that the AEA dosage was constant for all of the final mixtures, regardless of the type of aggregate or types and amounts of cementitious materials.

Another trend that can be observed in Table 9 is that final mixtures containing fly ash, regardless of pumicite or fly ash percentage, required more HRWRA (40.1-43.7 fl oz/yd^3 [1550-1690 mL/m^3]) to achieve the acceptable slump and air content than mixtures without fly ash (32.8-38.3 fl oz/yd^3 [1270-1480 mL/m^3]). This observation is contrary to the expectation that using fly ash would increase workability (or decrease the required HRWRA dosage) (*20*). However, fly ash is also known to decrease air content (*20*) and low air content of mixtures in this work were usually corrected by increasing HRWRA dosage. Therefore, if the increased HRWRA dosage, provided to improve AEA effectiveness, was greater than the decrease in HRWRA dosage that potentially could have been provided by the fly ash, then a net increase in HRWRA dosage in mixtures containing fly ash would not be surprising.

5.4. Compressive Strength

Average results from four compression tests conducted at both seven and 28 days for each concrete mixture are presented in Table 10 and Figure 14. The 28-day compressive strength of specimens containing 30% natural pozzolan was 5.0% and 15.6% less than the compressive strength of specimens containing 10% natural pozzolan for specimens produced with Moriarty and Placitas aggregates, respectively. Although SCMs are supposed to improve mechanical properties of concrete through a pozzolanic reaction between $Ca(OH)_2$ and SiO_2 in the presence of water to produce secondary CSH (52), it appears that any compressive strength benefits expected from the natural pozzolan are not fully developed in the first 28 days (*30, 53*). Other researchers have shown that the natural pozzolan is more reactive at later ages (beyond 180 days) (*31,36*).

Specimens containing 30% natural pozzolan had 7-day and 28-day compressive strengths that were comparable to strengths from specimens with 30% fly ash. This can be seen in Table 10, by comparing results from mixtures P-N30-F00 and P-N00-F30 and results from mixtures M-N30-F00 and M-N00-F30, respectively. For example, 28-day compressive strengths of Moriarty specimens containing 30% natural pozzolan and 30% fly ash were 4560 psi (31.4 MPa) and 4550 psi (31.4 MPa), respectively. This indicates that the natural pozzolan can be a desirable alternative for fly ash in terms of compressive strength.

For mixtures that contained both fly ash and natural pozzolan, increasing the fly ash content from 10% to 20% led to a decrease in compressive strength. The 28-day compressive strength of mixture P-N22-F10 (5220 psi [36.0 MPa]) was 14.0% greater than mixture P-N20-F20 (4490 psi [31.0 MPa]) and 28-day compressive strength of mixture M-N22-F10 (5290 psi [36.5 MPa]) was 8.1% greater than mixture M-N20-F20 (4860 psi [33.5 MPa]). This strength decrease appears to be caused by increasing the total SCM content to 40% of the cementitious materials.

Table 10. Compressive strength results.

Placitas			Moriarty		
Mixture	7-day Compressive strength psi (MPa)	28-day Compressive strength psi (MPa)	Mixture	7-day Compressive strength psi (MPa)	28-day Compressive strength psi (MPa)
P-N10-F00	4630 (31.9)	5410 (37.3)	M-N10-F00	4440 (30.6)	5550 (38.3)
P-N20-F00	4410 (30.4)	5200 (35.9)	M-N20-F00	4160 (28.7)	5360 (37.0)
P-N30-F00	3580 (24.7)	4560 (31.4)	M-N30-F00	3990 (27.5)	5270 (36.3)
P-N00-F30	3560 (24.5)	4550 (31.4)	M-N00-F30	3920 (27.0)	4950 (34.1)
P-N10-F15	3990 (27.5)	5340 (36.8)	M-N10-F15	4180 (28.8)	5490 (37.8)
P-N15-F10	3810 (26.3)	5250 (36.2)	M-N15-F10	4090 (28.2)	5420 (37.4)
P-N22-F10	3690 (25.4)	5220 (36.0)	M-N22-F10	4040 (27.9)	5290 (36.5)
P-N20-F20	3430 (23.6)	4490 (31.0)	M-N20-F20	3830 (26.4)	4860 (33.5)

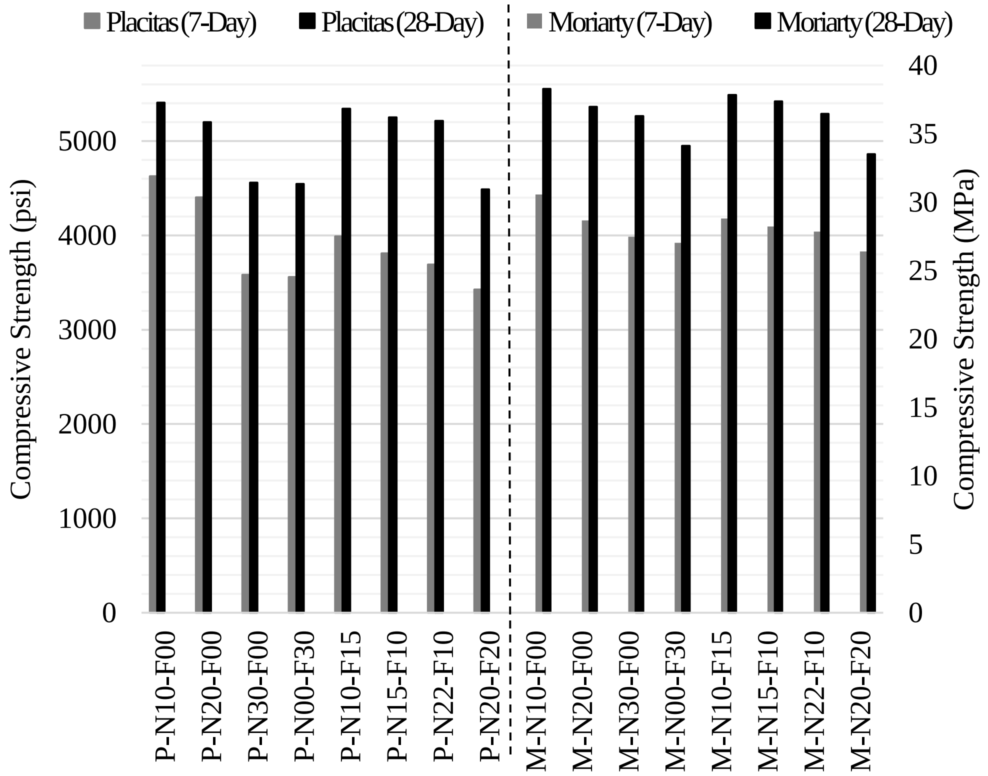

Figure 14. Compressive strength results.

5.5. Flexural Tests

Average MOR results from all beam specimens are presented in Table 11 and Figure 15. Specimens containing 30% natural pozzolan had MOR values that were less than comparable specimens with less pumicite. This rough trend of decreasing MOR with increasing pumicite content is consistent with the trend observed for compressive strength.

Specimens containing natural pozzolan were observed to have MOR values greater than 600 psi (4.14 MPa) and exceeded the flexural strengths provided by mixtures P-N00-F30 and M-N00-F30 that contained only fly ash, indicating that natural pozzolan can also be a good alternative for fly ash in terms of flexural strength.

Specimens produced with Moriarty aggregates had greater MOR values, by 4.5% on average, compared to similar Placitas specimens. These greater MOR values for Moriarty specimens are consistent with the greater compressive strengths from Moriarty specimens.

Table 11. Flexural strength results.

Placitas		Moriarty	
Mixture	28-day Modulus of rupture psi (MPa)	Mixture	28-day Modulus of rupture psi (MPa)
P-N10-F00	667 (4.60)	M-N10-F00	713 (4.92)
P-N20-F00	688 (4.74)	M-N20-F00	714 (4.92)
P-N30-F00	611 (4.21)	M-N30-F00	638 (4.40)
P-N00-F30	597 (4.12)	M-N00-F30	613 (4.23)
P-N10-F15	648 (4.47)	M-N10-F15	669 (4.61)
P-N15-F10	672 (4.63)	M-N15-F10	689 (4.75)
P-N22-F10	679 (4.68)	M-N22-F10	700 (4.83)
P-N20-F20	625 (4.31)	M-N20-F20	661 (4.56)

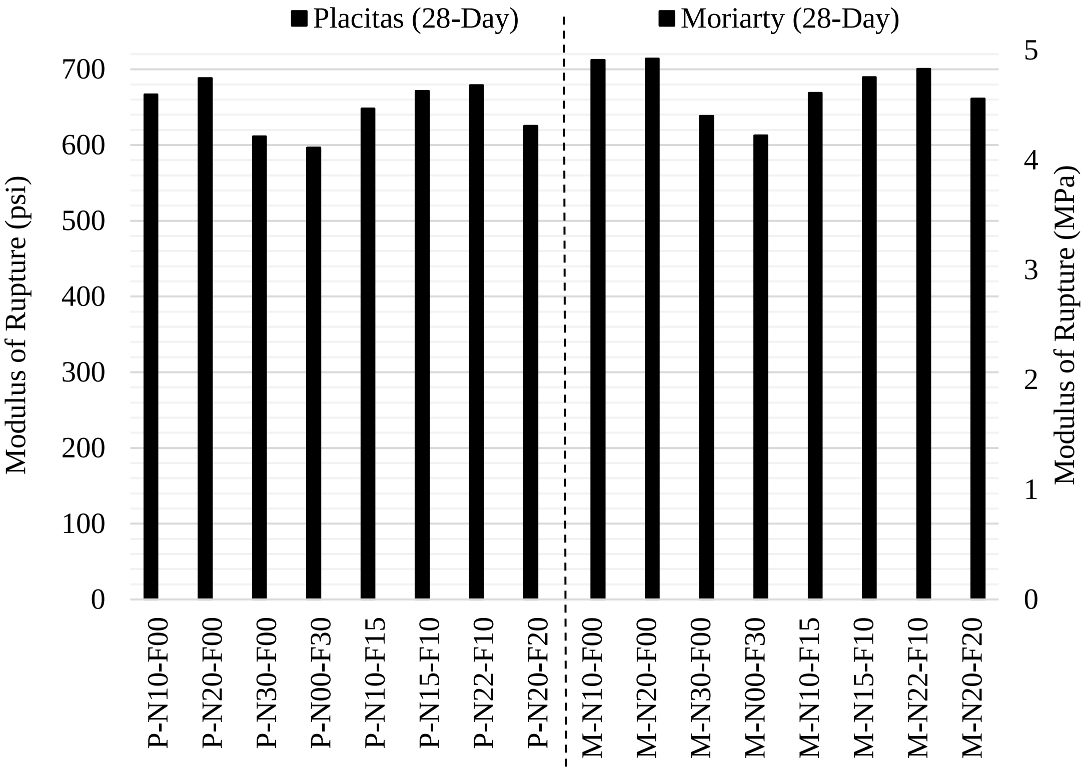

Figure 15. Flexural strength results.

5.6. Shrinkage

Average shrinkage results for four prism specimens from each concrete mixture are illustrated in Table 12 and Figures 16 and 17. The final shrinkage values for all mixtures were less than 710 μstrain, which is below the 800 μstrain maximum limit used by many state departments of transportation. It was also observed that shrinkage decreased as pumicite content increased, when fly ash was used in place of pumicite, and as the total SCM content increased. Mixtures P-N10-F00, P-N20-F00, and P-N30-F00 for Placitas aggregates and mixtures M-N10-F00, M-N20-F00, and M-N30-F00 for Moriarty aggregates show the trend of decreasing shrinkage with increasing pumicite content. Mixtures containing 30% fly ash (P-N00-F30 and M-N00-F30) exhibited less shrinkage than mixtures containing 30% natural pozzolan (P-N30-F00 and M-N30-F00). The 30% fly ash mixtures produced 21.1% and 31.7% less shrinkage than 30% pumicite mixtures for the Placitas and Moriarty aggregates, respectively. Finally, mixtures with the greatest SCM contents (P-N20-F20 and M-N20-F20) experienced the least shrinkage.

As can be seen in Table 12 and Figures 16 and 17, results for Placitas mixtures with 25% and 32.5% SCM (P-N10-F15, P-N15-F10, P-N22-F10) do not seem to follow the overall trend of decreasing shrinkage with increasing SCM content and also seem to contradict the results for the corresponding Moriarty mixtures (M-N10-F15, M-N15-F10, M-N22-F10). This contradictory behavior indicates that the trends across a narrow range of SCM contents (25% to 32.5% total SCM content) are not strong in comparison to the variation in the measurements. In other words, the variation is greater than the strength of the trends across these mixtures.

Table 12. Final shrinkage test results.

Placitas		Moriarty	
Mixture	Final Shrinkage (μstrain)	Mixture	Final Shrinkage (μstrain)
P-N10-F00	709	M-N10-F00	675
P-N20-F00	683	M-N20-F00	674
P-N30-F00	667	M-N30-F00	642
P-N00-F30	526	M-N00-F30	439
P-N10-F15	559	M-N10-F15	548
P-N15-F10	631	M-N15-F10	537
P-N22-F10	595	M-N22-F10	531
P-N20-F20	462	M-N20-F20	409

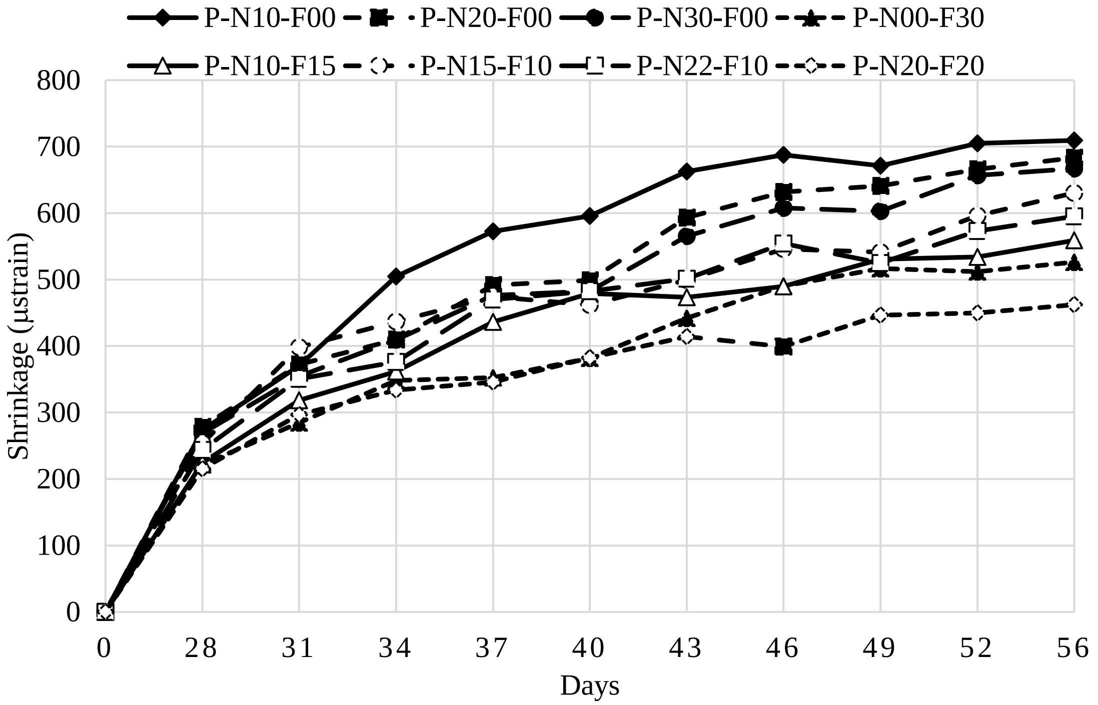

Figure 16. Shrinkage test results (Placitas aggregate).

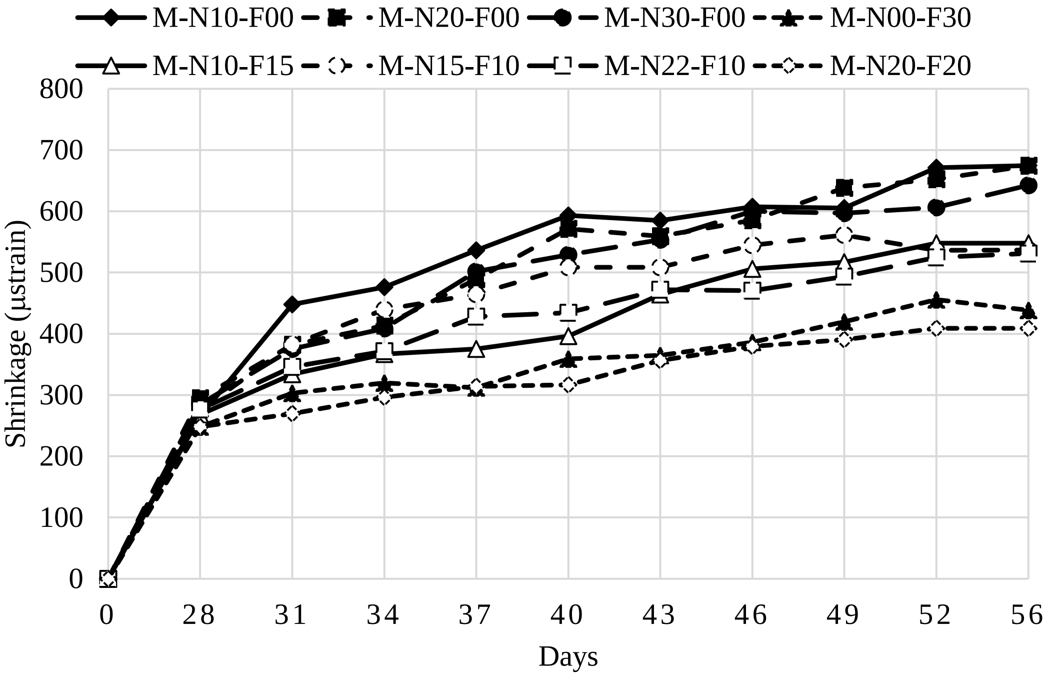

Figure 17. Shrinkage test results (Moriarty aggregate).

5.7. Freezing and Thawing

Results for freezing and thawing tests are presented in Table 13 and Figures 18 and 19. Mixtures containing only 10% pumicite were not evaluated through freezing and thawing tests because these mixtures were shown to be unacceptable for ASR mitigation. DF values (RDM after 300 cycles) for all other mixtures were greater than 75, indicating that they are acceptable according to ASTM C666 (*48*) (DF greater than 60). These results show that an adequate air void system was produced for each acceptable combination of cementitious materials and admixture dosages.

The results also show that the mixtures containing 20 and 30% pumicite had the lowest DF values for both aggregate sources, and these DF values were significantly less than the DFs obtained using 30% fly ash. These results are consistent with observations by Öz (*39*) that mixtures with 30% natural pozzolan had low DF. The specific cause of the lower DFs for the pumicite mixtures was not investigated, so it is important to note that the lower DFs may have been caused by a specific interaction with one or both of the admixtures used in this study. Alternatively, the natural pozzolan may cause the air void system to have a different distribution (pore size or spacing), although a hardened air void analysis (ASTM C457 [*54*]) would need to perform to verify this.

As can be seen in Table 13 and Figures 18 and 19, increasing SCM content in concrete mixtures containing both fly ash and pumicite increased DF. Specifically, the trend for increasing DF with increasing SCM content is demonstrated by ordering mixtures with 25% SCM (P-N10-F15, P-N15-F10, M-N10-F15, and M-N15-F10) that had the lowest DF values, mixtures with 32.5% SCM (P-N22-F10 and M-N22-F10) that had intermediate DF values, and mixtures with 40% SCM (P-N20-F20 and M-N20-F20) that had the greatest DF values.

Table 13. Freezing and thawing test results.

Placitas		Moriarty	
Mixture	DF (300-cycle RDM)	Mixture	DF (300-cycle RDM)
P-N10-F00	NA	M-N10-F00	NA
P-N20-F00	80.7	M-N20-F00	78.7
P-N30-F00	81.5	M-N30-F00	79.3
P-N00-F30	89.1	M-N00-F30	84.8
P-N10-F15	85.2	M-N10-F15	83.0
P-N15-F10	84.3	M-N15-F10	82.5
P-N22-F10	87.7	M-N22-F10	85.2
P-N20-F20	89.8	M-N20-F20	86.4

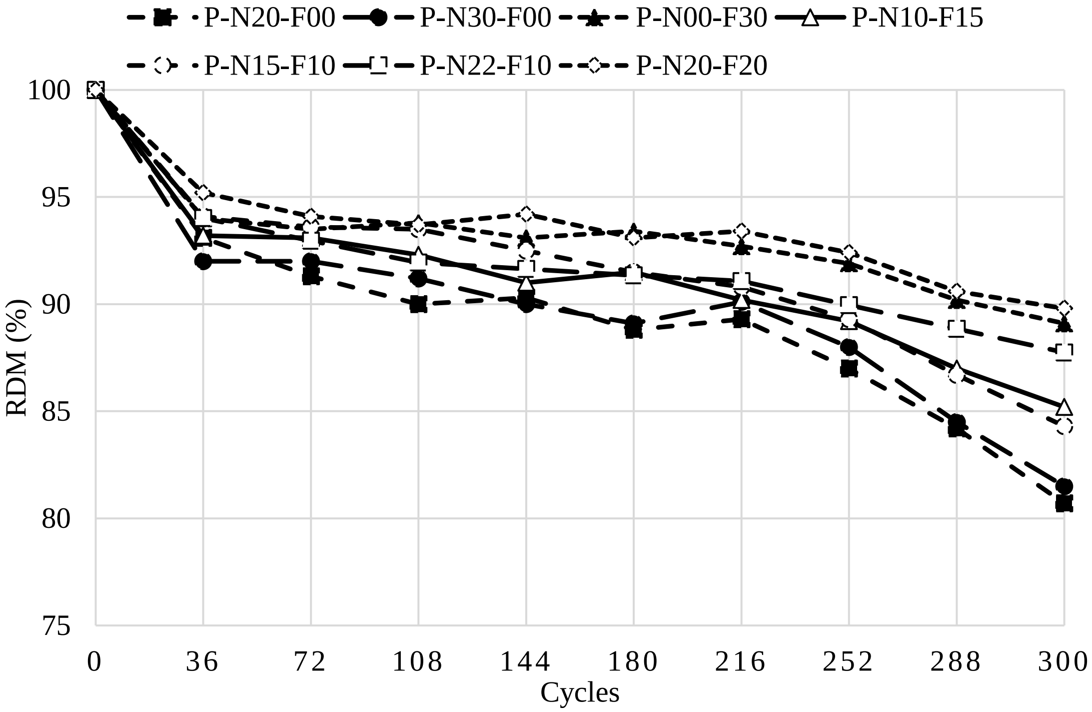

Figure 18. Freezing and thawing test results (Placitas aggregate).

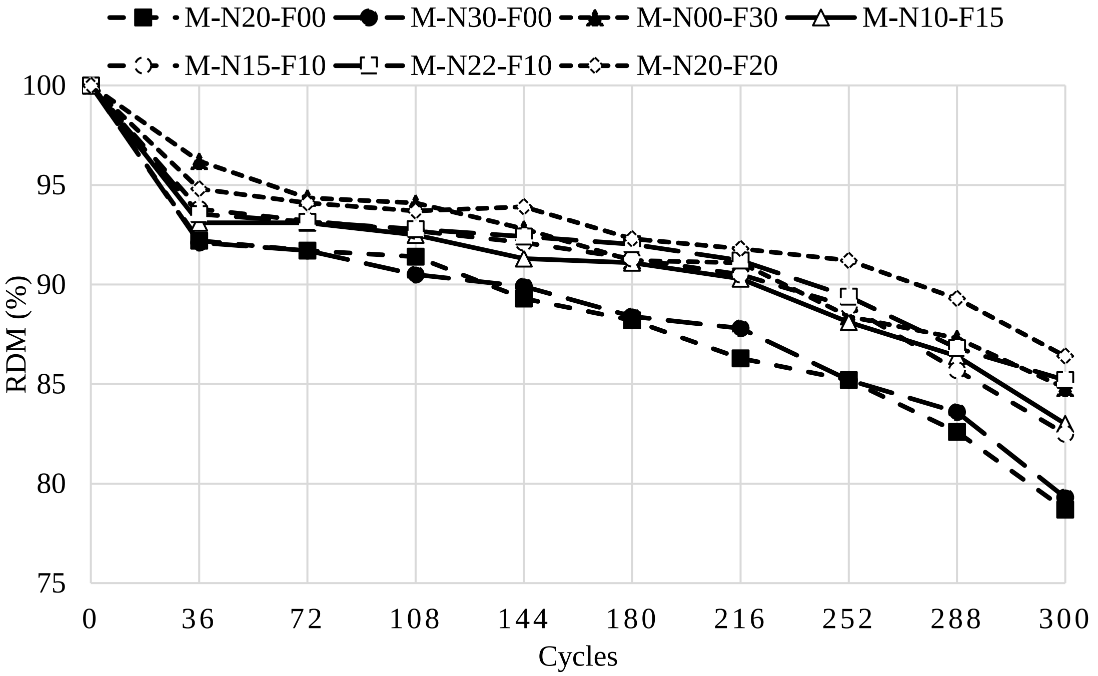

Figure 19. Freezing and thawing test results (Moriarty aggregate).

5.8. Rapid Chloride Permeability Test

During the course of this project, a vacuum pump required for pre-conditioning the specimens needed to be replaced. This equipment issue caused the RCPT to be delayed until the specimens were 150 days old. This testing age is acceptable since ASTM C1202 (*50*) recommends at least 56 days of moist curing for specimens containing SCMs. According to ASTM C1202 (*50*), concrete specimens containing SCMs may continue to show reductions in results of this test beyond 56 days, and in some cases, it may be appropriate to test at later ages. Testing at later ages allows slow reacting SCMs to react more completely and provides a better indication of the long-term durability of a concrete mixture containing a SCM.

The 150-day RCPT results are presented in Table 14 and Figure 20. In this study, the RCPT results (total charge passed) for all mixtures ranged from 302 to 592 coulombs. According to Table 1, RCPT results between 100 and 1000 coulombs indicate that the chloride ion penetration is very low. Therefore, all concrete mixtures used in this study were categorized as having very low chloride ion penetration. Mixtures with 40% SCM had the lowest charge passed during RCPT for both aggregate sources. This is most likely due to additional secondary CSH formation, resulting from reaction of the SCMs, decreasing permeability of the mixtures (*52*, *55*).

Table 14. RCPT results.

Placitas		Moriarty	
Mixture	Total charge passed (coulombs)	Mixture	Total charge passed (coulombs)
P-N10-F00	592	M-N10-F00	562
P-N20-F00	478	M-N20-F00	468
P-N30-F00	366	M-N30-F00	343
P-N00-F30	331	M-N00-F30	305
P-N10-F15	349	M-N10-F15	309
P-N15-F10	356	M-N15-F10	345
P-N22-F10	385	M-N22-F10	347
P-N20-F20	302	M-N20-F20	306

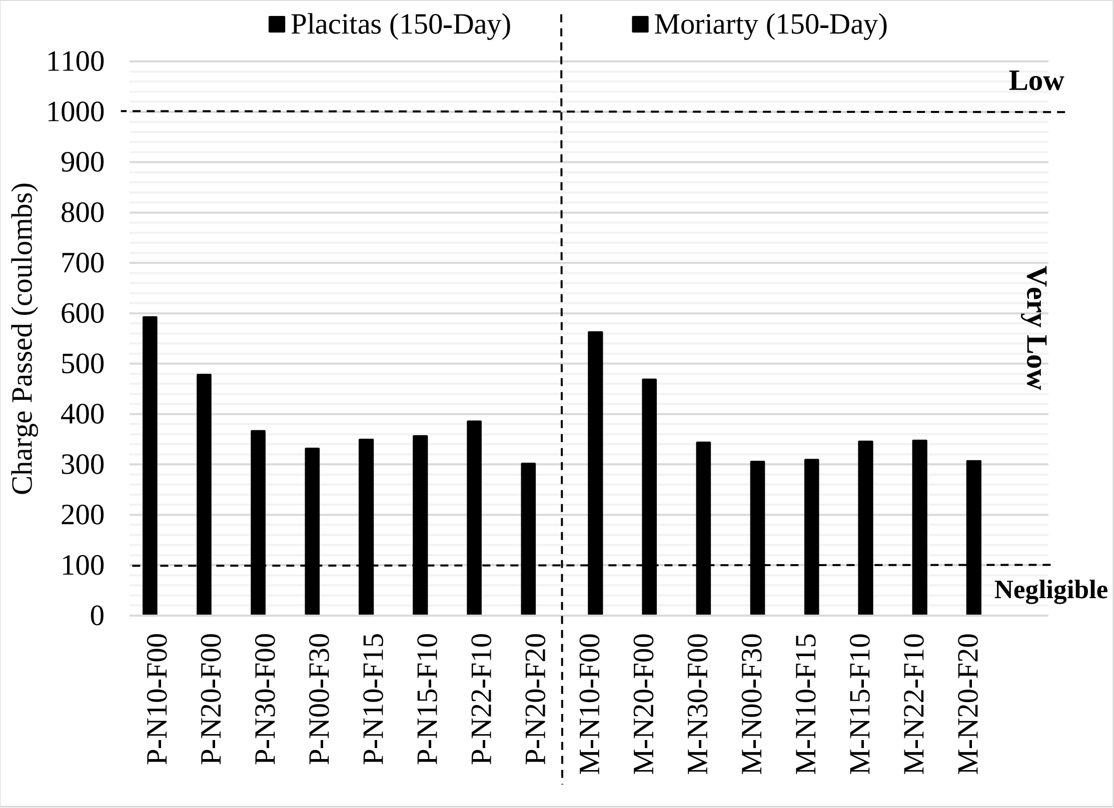

Figure 20. RCPT test results.

The RCPT results also show that increasing pumicite content from 10% to 30% improved resistance to chloride ion penetration, showing the effectiveness of pumicite in preventing chloride ion ingress into concrete. Additionally, comparing specimens containing 30% fly ash and specimens containing 30% pumicite shows that using fly ash resulted in a lower charge passed for both Placitas and Moriarty aggregates. However, the benefit of using fly ash is not substantial and should not cause any concern about replacing fly ash with pumicite.

As can be seen in Table 14 and Figure 20, increasing SCM content in concrete mixtures containing both fly ash and pumicite did not show a significant trend. The RCPT results for mixtures P-N10-

F15, P-N15-F10, P-N22-F10, and P-N20-F20 had similar results, as did mixtures M-N10-F15, M-N15-F10, M-N22-F10, and M-N20-F20.

Although RCPT is widely used due to its short duration and convenience, the test has the following drawbacks:

1. The high voltage used during RCPT leads to an increase in temperature that can cause conservative but misleading results for normal concrete. However, the increased temperature can cause RCPT to overestimate the chloride ion resistance of mixtures containing SCMs (56).

2. RCPT results may not represent the true chloride permeability for concrete that contains SCMs or chemical admixtures. Adding pozzolans to concrete reduces the OH- concentration of the pore solution (*17, 62*). The reduced ionic concentration of the pore solution can cause artificially low total charge passed measurements for RCPT when concrete mixtures contain SCMs. (*56, 57, 63*-*65*).

3. RCPT results are known to have greater variability than results from surface resistivity tests (*57*). The ASTM C1202 (*50*) statement on precision, based on work by Mobasher and Mitchell (*65*), states that two properly conducted tests may vary by as much as 35% if performed by the same person.

5.9. Surface Resistivity

Surface resistivity tests were performed at 28 days and 180 days. The 28-day surface resistivity tests were performed as part of the original project schedule while the 180-day tests were conducted to provide a comparison for the 150-day RCPT results. Results of 28-day and 180-day surface resistivity tests are provided in

Table 15 and in Figures 21 and 22. The results indicate that increasing pumicite content from 10% to 30% improved both 28-day and 180-day resistance to chloride ion penetration. The improved resistance to chloride ion penetration with increasing pumicite content is most likely due to greater density caused by either the pumicite particle sizes or the pozzolanic reaction of pumicite. Specifically, secondary CSH formation resulting from the natural pozzolan reacting with $Ca(OH)_2$ can fill pore spaces between cement particles, decreasing permeability of the mixture (*52, 55)*.

Table 15. Surface resistivity results.

Placitas			Moriarty		
Mixture	28-day surface resistivity kΩ-in. (kΩ-mm)	180-day surface resistivity kΩ-in. (kΩ-mm)	Mixture	28-day surface resistivity kΩ-in. (kΩ-mm)	180-day surface resistivity kΩ-in. (kΩ-mm)
P-N10-F00	6.22 (158)	14.0 (355)	M-N10-F00	6.04 (153)	13.7 (348)
P-N20-F00	8.50 (216)	14.6 (371)	M-N20-F00	8.73 (222)	15.0 (379)
P-N30-F00	10.02 (255)	15.7 (398)	M-N30-F00	9.48 (241)	15.1 (382)
P-N00-F30	5.92 (150)	16.0 (406)	M-N00-F30	6.89 (175)	16.1 (409)
P-N10-F15	7.32 (186)	14.87 (378)	M-N10-F15	8.39 (213)	15.8 (400)
P-N15-F10	7.44 (189)	14.6 (371)	M-N15-F10	8.15 (207)	15.5 (394)
P-N22-F10	7.82 (199)	15.0 (382)	M-N22-F10	8.62 (219)	16.0 (405)
P-N20-F20	8.09 (206)	16.8 (427)	M-N20-F20	9.00 (229)	16.5 (419)

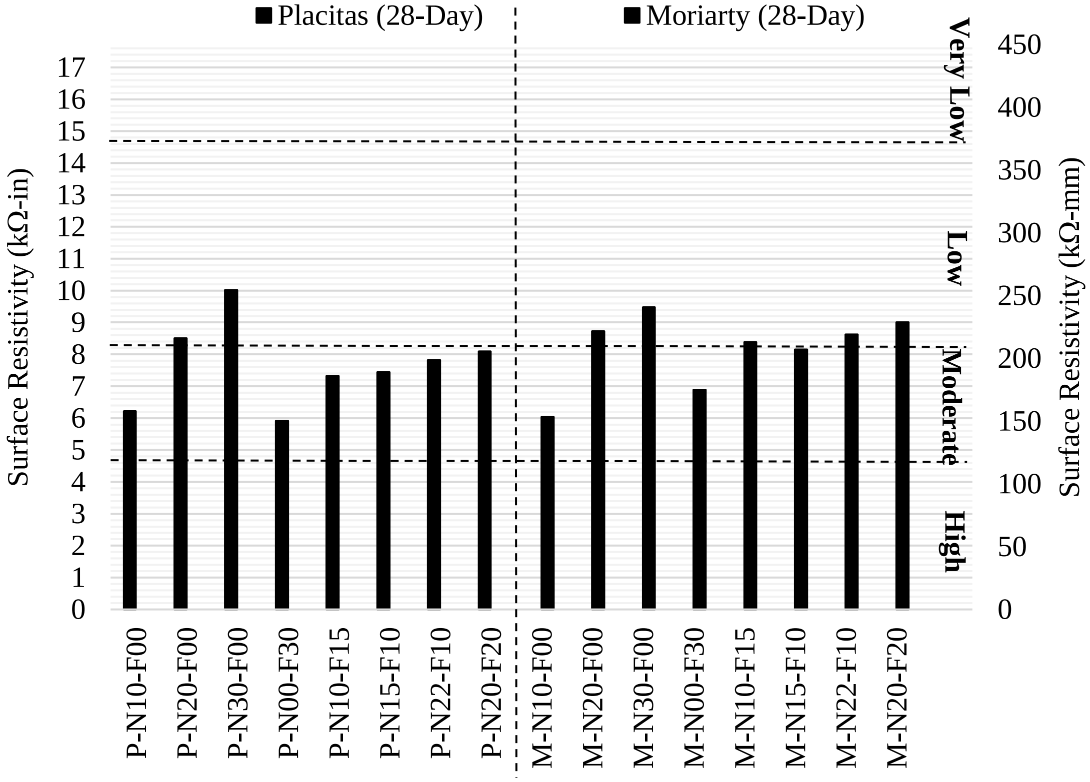

Figure 21. 28-day surface resistivity test results.

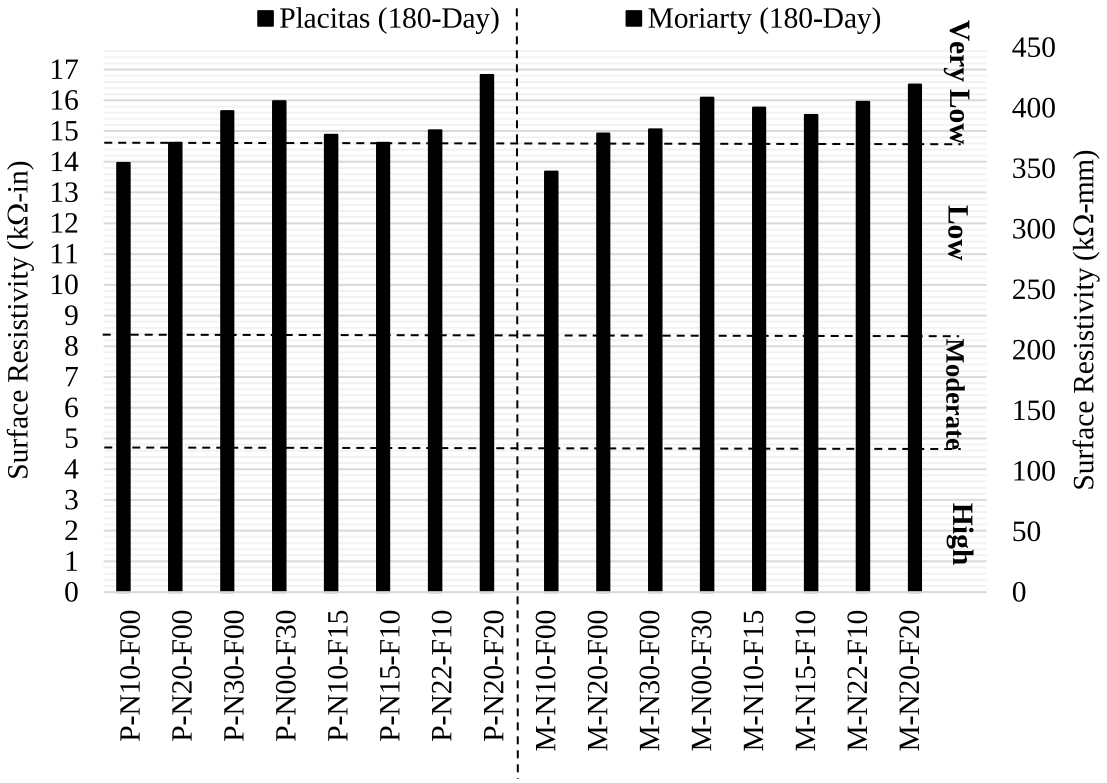

Figure 22. 180-day surface resistivity test results.

The 28-day surface resistivity results also show that the mixtures that were most susceptible to chloride ion penetration were the mixtures that contained either 10% natural pozzolan or 30% fly ash for both Placitas and Moriarty aggregates. Although these mixtures had the lowest 28-day surface resistivities, they provided moderate chloride ion resistance and would be appropriate for use in many applications. In contrast, results from testing at 180 days show that the surface resistivities of the concrete mixtures containing 30% fly ash improved dramatically relative to other mixtures. After 180 days, surface resistivities of 30% fly ash mixtures were 170% and 134% greater than their 28-day values for Placitas and Moriarty aggregates, respectively, making them two of the least susceptible mixtures to chloride ion penetration. At 180 days, the 30% fly ash mixtures even had greater resistance to chloride ion penetration than mixtures containing 30% pumicite. The values in

Table 15 indicate that 30% natural pozzolan mixtures provided much better surface resistivities than 30% fly ash mixtures at 28 days, while the 30% fly ash mixtures provided slightly better long-term surface resistivities. The drastic improvement of the 30% fly ash mixtures between 28 and 180 days shows the slow reaction of the fly ash.

In general, increasing SCM content (from 10% pumicite to 40% total SCM) increased 180-day surface resistivity values. This trend is not particularly clean for the 180-day tests, and it is important to note that this trend did not exist in the 28-day results. The lack of trend in the 28-day results is partially due to the fly ash not having reacted completely at 28 days.

Table 15 and Figures 21 and 22 also show that Placitas and Moriarty specimens containing both fly ash and natural pozzolan had slightly reduced 28-day surface resistivities compared to specimens containing 20% or 30% pumicite and no fly ash. However, the 180-day results show that the difference between surface resistivities of specimens containing both fly ash and pumicite and surface resistivities of specimens containing 20% or 30% pumicite and no fly ash is small. The improved surface resistivities of the fly ash mixtures from 28 to 180 days again indicates that the fly ash reacts slowly, but at later ages, fly ash and pumicite provide similar resistance to chloride ion penetration.

This increased surface resistivities at 180 days caused many of the concrete mixtures to move from the moderate chloride ion penetration category (at 28 days) to the very low chloride ion penetration category (at 180 days). This matches well with the 150-day RCPT results where all of the concrete mixtures were categorized as having very low chloride ion penetration.

Other researchers have shown that the surface resistivity test results correlate well with RCPT results (*66*, *67*). As can be seen in Figure 23, the surface resistivity and RCPT results from this study compare reasonably well with Equation 11 developed by El Dieb (*66*):

$$\mathrm{TCP} = 26068 \times SR^{-1.097} \qquad [11]$$

where:
TCP = total charge passed during an RCPT (coulombs); and
SR = surface resistivity measurement (kΩ-cm).

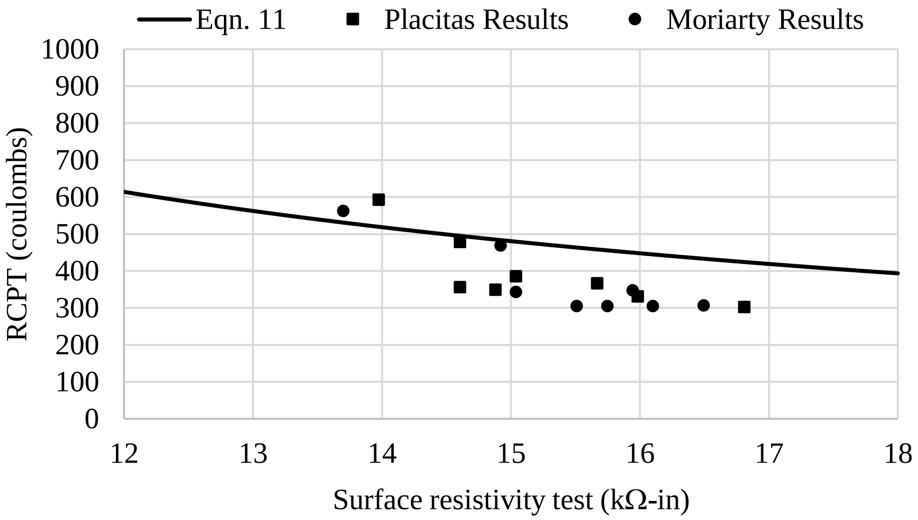

Figure 23. Relationship between surface resistivity and RCPT results.

Comparing the RCPT and surface resistivity tests shows that the surface resistivity test has several advantages. These advantages include:

1. A surface resistivity test takes approximately 30 minutes to perform, whereas RCPT requires approximately 30 hours to pre-condition a sample and run the test.
2. Surface resistivity tests can be conducted in-situ, while RCPT requires a sample to be cut from a concrete specimen or member and the test can only be performed under laboratory conditions.
3. Surface resistivity can be measured at low voltages, and this voltage is only applied for brief periods. This avoids errors resulting from heating of the concrete that commonly occur during RCPT (*68*).

6. CONCLUSIONS

Based on the research conducted during the course of this project, the following conclusions were drawn:

1. A minimum natural pozzolan content of 20% is needed to effectively mitigate ASR.
2. Mortar mixtures containing 30% natural pozzolan had approximately 40% less expansion than mortar mixtures containing 30% fly ash, indicating that the natural pozzolan was substantially more effective at mitigating ASR than fly ash.
3. Ternary mixtures containing both natural pozzolan and fly ash were the most effective mixtures for mitigating ASR expansion.
4. In terms of controlling ASR, the natural pozzolan appears to be suitable for completely replacing fly ash. However, negligible expansion can be achieved by maintaining a fly ash content of 10% when fly ash is available.
5. Workability of all mixtures were consistent enough to achieve acceptable slumps in relatively few attempts (no more than two adjustments to the HRWRA and AEA were needed).
6. Air content of the concrete mixtures was usually adjusted by changing HRWRA and AEA dosages to achieve an acceptable air content with just a few attempts.
7. A decrease of 15.6% was observed in the 28-day compressive strength of specimens containing 30% natural pozzolan compared to specimens containing 10% pumicite.
8. Specimens containing 30% natural pozzolan had 7-day and 28-day compressive strengths comparable to strengths of specimens with 30% fly ash. This indicates that natural pozzolan can be a desirable alternative for fly ash in terms of compressive strength.
9. Every beam specimen containing the natural pozzolan had a MOR greater than 600 psi (4.14 MPa) and exceeded the flexural strengths provided by mixtures that contained only fly ash, indicating that pumicite can also be a good alternative for fly ash in terms of flexural strength.
10. Final shrinkage values for all of the concrete mixtures were less than 710 μstrain, which is below the 800 μstrain maximum limit used by many state departments of transportation. More specific conclusions that can be drawn from the shrinkage results include:
    a. Increasing pumicite content from 10 to 30% decreased shrinkage.
    b. Mixtures containing 30% fly ash had at least 20% less shrinkage than mixtures containing 30% pumicite.
    c. Mixtures with the greatest SCM contents (40%) experienced the least shrinkage.
11. From the freezing and thawing tests, DF values for all mixtures were greater than 75, indicating that they were acceptable according to ASTM C666 (*48*). More specific conclusions that can be drawn from the freezing and thawing results include:

    a. Mixtures containing 20 and 30% pumicite had the lowest DF values for both aggregate sources.
    b. DF values for mixtures with 30% fly ash were significantly greater than the DFs obtained for mixtures with 30% pumicite.
    c. Mixtures containing both fly ash and pumicite showed a general trend of increasing DF with increased total SCM content.

12. RCPT showed that all concrete mixtures used in this study had total charge passed less than 600 coulombs (very low chloride ion penetration). More specific conclusions that can be drawn from the RCPT results include:
    a. Increasing pumicite content decreased chloride ion penetration in RCPT, indicating that pumicite can effectively prevent chloride ion ingress into concrete.
    b. Using 30% fly ash resulted in a lower charge passed than using 30% natural pozzolan for both Placitas and Moriarty aggregates. However, the benefit of using fly ash was not substantial and should not cause any concern about replacing fly ash with pumicite.
    c. Mixtures containing 40% SCM had the greatest resistance to chloride ion penetration.
13. Measured surface resistivity values at 180 days were much greater than 28-day surface resistivities, moving almost all specimens from the moderate category (at 28 days) to the very low chloride ion penetration category (at 180 days). More specific conclusions that can be drawn from the surface resistivity results include:
    a. Increasing pumicite content from 10% to 30% improved both 28-day and 180-day resistance to chloride ion penetration.
    b. Mixtures containing 30% fly ash provided substantially less chloride ion penetration resistance than 30% natural pozzolan mixtures at 28 days, but slightly better chloride resistance at 180 days.
    c. Increasing SCM content, from 10% pumicite to 40% total SCM, increased 180-day surface resistivity values. However, this trend was not strong and did not exist in the 28-day results.
14. The 180-day surface resistivity measurements were mostly consistent with the RCPT results in terms of comparing their chloride ion penetration resistance categories. The surface resistivity and RCPT results were also reasonably consistent with established correlations.

REFERENCES

1. Dhir, R. K., J. G. L. Munday, and L. T. Ong. Investigations of the Engineering Properties of OPC/Pulverized-Fuel Ash Concrete: Deformation Properties. *The Institution of Structural Engineers*, 1986. 64B2: 36-42.

2. Atis, C. D., A. Kilic, and U. K. Sevim. Strength and Shrinkage Properties of Mortar Containing a Nonstandard High-Calcium Fly Ash. *Cement and Concrete Research*, 2004. 34 (1): 99-102.

3. Stanton, T. E. Expansion of Concrete Through Reaction Between Cement and Aggregate. *Proceedings of the American Society of Civil Engineers*, Vol. 66, New York, 1940, pp. 1781 to 1811.

4. Poole, A. B. Introduction to Alkali-Aggregate Reaction in Concrete. In the *Alkali-Silica Reaction in Concrete* (Edited by Swamy, R. N., and R. Van Nostrand), New York, New York, 1992, pp.1-28.

5. Thomas, M. D. A., B. Fournier, and K.J. Folliard. *Alkali-Aggregate Reactivity (AAR) Facts Book*. Public FHWA-HIF-13-019. FHWA, U.S. Department of Transportation, 2013.

6. Farney, J. A., and B. Kerkhoff. Diagnosis and Control of Alkali-Aggregate Reactions in Concrete. *Portland Cement Association*, 2007.

7. Folliard, K. J, M. D. A. Thomas, and K. E. Kurtis. *Guidelines for The Use of Lithium to Mitigate or Prevent Alkali-Silica Reaction (ASR): Chapter 2 Alkali-Silica Reaction*. Public FHWA-RD-03-047. FHWA, U.S. Department of Transportation, 2003.

8. Sims, I., A. Poole. *Alkali-Aggregate Reaction in Concrete - A World Review*. CRC Press, 2017.

9. Schalm, O., and W. Anaf. Laminated Altered Layers in Historical Glass: Density Variations of Silica Nanoparticle Random Packings as Explanation for the Observed Lamellae. *Journal of Non-Crystalline Solids*, 2016. 442: 1-16.

10. Multon, S., M. Cyr, A. Sellier, A. Leklou, and L. Petit. Coupled Effects of Aggregate Size and Alkali Content on ASR Expansion. *Cement and Concrete Research*, 2007. 38 (3), 350-359.

11. Steffens, A., K. Li, and O. Coussy. Aging Approach to Water Effect on Alkali-Silica Reaction Degradation of Structures. *Journal of Engineering Mechanics*, 2002. 129 (1): 50-59.

12. Stark, D. The Moisture Condition of Field Concrete Exhibiting Alkali-Silica Reactivity. *Durability of Concrete: Second International Conference*, 1991, 2: 973-987.

13. Snellings, R. Assessing, Understanding and Unlocking Supplementary Cementitious Materials. *RILEM Technical Letters*, 2016. 1: 50-55.

14. American Coal Ash Association (ACAA). Fly Ash Use in Concrete Increases Slightly as Overall Coal Ash Recycling Rate Declines, 2020.

15. Malvar, L. J., and L. R. Lenke. Efficiency of Fly Ash in Mitigating Alkali-Silica Reaction Based on Chemical Composition. *American Concrete Institute Materials Journal*, 2006, 103(5): 319-326.

16. Joshi, P., and C. Chan. Rapid Chloride Permeability Testing. *Hanley-Wood, LLC.* 2002. Publication #C02L037.

17. Stanish, K. D., R. D. Hooton, and M. D. A. Thomas. *Testing the Chloride Penetration Resistance of Concrete: A Literature Review*. FHWA, U.S. Department of Transportation, 1997.

18. Portland Cement Association (PCA). Freeze-Thaw Resistance. https://www.cement.org/Learn/concrete-technology/durability/freeze-thaw-resistance. Accessed October 25, 2021.

19. Reiterman, P., O. Holčapek, O. Zobal, and M. Keppert. Freeze-Thaw Resistance of Cement Screed with Various Supplementary Cementitious Materials. *Reviews on Advanced Materials Science*, 2019. 58(1): 66-74.

20. Kosmatka, S. H., and M. L. Wilson. Design and Control of Concrete Mixtures. Portland Cement Association (15th Edition), 2011.

21. Hill, R. L., and K. L. Folliard. *The Impact of Fly Ash on Air-Entrained Concrete*. Concrete, tech talk, pp. 71-72. 2006.

22. Tanesi, J. and R. Meininger. *Freeze-Thaw Resistance of Concrete with Marginal Air Content*. Public FHWA-HRT-06-117. FHWA, U.S. Department of Transportation, 2006.

23. Holt, E. E. Early Age Autogenous Shrinkage of Concrete. *VTT Technical Research Center of Finland*, 2001.

24. Papayianni, I., F. Kesikidou, and P. H. Alt. The Role of Shrinkage Reducing Admixtures and Supplementary Cementitious Materials in Volume Stability and Strength Development. *MATEC Web of Conferences*, 2019. 289.

25. Kristiawan, S., and M. T. M., Aditya. Effect of High-Volume Fly Ash on Shrinkage of Self-compacting Concrete. *Procedia Engineering*, 2015. 125: 705-712.

26. Sutter, L. L. *Supplementary Cementitious Materials - Best Practices for Concrete Pavements.* Public FHWA-HIF-16-001. FHWA, U.S. Department of Transportation, 2016.

27. ASTM C618-19: *Standard Specification for Coal Fly Ash and Raw or Calcined Natural Pozzolan for Use in Concrete*. Annual Book of ASTM Standards. ASTM International, West Conshohocken, PA, 2019.

28. Spears, D. A., J. H. Sharp, D. Thompson, and B. B. Argent. Prediction of the Phases Present in Fly Ash, Their Composition and the Influence of These Factors on Its Utility and Disposal. *Proceedings of The Institute of Energy Conference*, London, UK, (December 1995). 71-87.

29. Sudarsan, V. *Materials Under Extreme Conditions*, Elsevier, ISBN: 9780128013007. Chapter 4 - Materials for Hostile Chemical Environments, 2017. 129-158.

30. Khandaker, M., A. Hossain. Properties of Volcanic Pumice Based Cement and Lightweight. *Cement and Concrete Research*, 2004. 34(2): 283-291.

31. *K*abay, N., M. M. Tufekci, A. B. Kizilkanat, and D. Oktay. Properties of Concrete with Pumice Powder and Fly Ash as Cement Replacement Materials. *Construction and Building Materials*, 2015. 85: 1-8.

32. Hossain, K. M. A. Blended Cement Using Volcanic Ash and Pumice. *Cement and Concrete Research*, 2003. 33 (10): 1601-1605.

33. Ramasamy, U., A. C. Bordelon, and P. J. Tikalsky. Properties of Different Pumice Grades Blended with Cement. *Journal of Materials in Civil Engineering (ASCE),* 2017. 29 (7).

34. Liu, J., X. J. Lv, M. L. Cao, and S. C. Cui. Experimental Study on Cementitious Property of Pumice. *Applied Mechanics and Materials*, 2011. 99–100: 773-776.

35. Sarıdemir, M. Effect of Silica Fume and Ground Pumice on Compressive Strength and Modulus of Elasticity of High Strength Concrete. *Construction and Building Materials*, 2013. 49: 484-489.

36. Zeyad, A. M., B. A. Tayeh, and M. O. Yusuf. Strength and Transport Characteristics of Volcanic Pumice Powder Based High Strength Concrete. *Construction and Building Materials*, 2019. 216: 314-3324.

37. Tangtermsirikul, S., and P. Kitticharoenkiat. Development of Low Heat Concrete Using Fly Ash and Pumicite. *Research and Development Journal of the Engineering Institute of Thailand*, 1997. 1: 88-98.

38. Granata, M. F. Pumice Powder as Filler of Self-Compacting Concrete. *Construction and Building Materials*, 2015. 96: 581-590.

39. Öz, H. Ö., H. E. Yücel, and M. Günes. Freeze-Thaw Resistance of Self Compacting Concrete Incorporating Basic Pumice. *International Journal of Theoretical and Applied Mechanics*, 2016. 1: 285-291.

40. ASTM C1567-21: *Standard Test Method for Determining the Potential Alkali-Silica Reactivity of Combinations of Cementitious Materials and Aggregate (Accelerated Mortar-Bar Method),* Annual Book of ASTM Standards. ASTM International, West Conshohocken, PA, 2014.

41. ASTM C192/C192M-19: *Standard Practice for Making and Curing Concrete Test Specimens in the Laboratory*. Annual Book of ASTM Standards. ASTM International, West Conshohocken, PA, 2019.

42. ASTM C511-19*, Standard Specification for Mixing Rooms, Moist Cabinets, Moist Rooms, and Water Storage Tanks Used in the Testing of Hydraulic Cements and Concretes.* Annual Book of ASTM Standards ASTM International, West Conshohocken, PA, 2019.

43. ASTM C143/C143M-20: *Standard Test Method for Slump of Hydraulic-Cement Concrete*. Annual Book of ASTM Standards. ASTM International, West Conshohocken, PA, 2020.

44. ASTM C231/C231M-17a: S*tandard Test Method for Air Content of Freshly Mixed Concrete by the Pressure Method*. Annual Book of ASTM Standards. ASTM International, West Conshohocken, PA, 2017.

45. ASTM C39/C39M-21: *Standard Test Method for Compressive Strength of Cylindrical Concrete Specimens*. Annual Book of ASTM Standards. ASTM International, West Conshohocken, PA, 2021.

46. ASTM C78/C78M-21: *Standard Test Method for Flexural Strength of Concrete (Using Simple Beam with Third-Point Loading).* Annual Book of ASTM Standards. ASTM International, West Conshohocken, PA, 2021.

47. ASTM C157/C157M-08: *Standard Test Method for Length Change of Hardened Hydraulic-Cement Mortar and Concrete.* Annual Book of ASTM Standards. ASTM International, West Conshohocken, PA, 2017.

48. ASTM C666/C666M-03: *Standard Test Method for Resistance of Concrete to Rapid Freezing and Thawing*. Annual Book of ASTM Standards. ASTM International, West Conshohocken, PA, 2015.

49. ASTM C215-19: *Standard Test Method for Fundamental Transverse, Longitudinal, and Torsional Resonant Frequencies of Concrete Specimens*. Annual Book of ASTM Standards. ASTM International, West Conshohocken, PA, 2019.

50. ASTM C1202-12: *Standard Test Method for Electrical Indication of Concrete's Ability to Resist Chloride Ion Penetration*. Annual Book of ASTM Standards. ASTM International, West Conshohocken, PA, 2019.

51. AASHTO T 358: *Standard Method of Test for Surface Resistivity Indication of Concrete's Ability to Resist Chloride Ion Penetration*. Washington, D.C., 2019.

52. Ezziane, K., A. Bougara, A. Kadri, H. Khelafi, and E. Kadri. Compressive Strength of Mortar Containing Natural Pozzolan Under Various Curing Temperature. *Cement and Concrete Composites*, 2007. 29 (8): 587-593.

53. Khandaker, M., and A. Hossain. Potential Use of Volcanic Pumice as a Construction Material. *Journal of Materials in Civil Engineering (ASCE),* 2004. 16 (6): 573-577.

54. ASTM C457/C457M-16: *Standard Test Method for Microscopical Determination of Parameters of the Air-Void System in Hardened Concrete*. Annual Book of ASTM Standards. ASTM International, West Conshohocken, PA, 2016.

55. Lam, L., Y. L. Wong, and C. S. Poon. Degree of Hydration and Gel/Space Ratio of High-Volume Fly Ash/Cement Systems. *Cement and Concrete Research*, 2000. 30 (5): 747-756.

56. Bagheri, A. R., and H. Zanganeh. Comparison of Rapid Tests for Evaluation of Chloride Resistance of Concretes with Supplementary Cementitious Materials. *Journal of Materials in Civil Engineering (ASCE)*, 2012. 24 (9).

57. Shi, C. Effect of mixing proportions of concrete on its electrical conductivity and the rapid chloride permeability test (ASTM C1202 or ASSHTO T277) results. *Cement and Concrete Research*, 2004. 34 (3): 537-545.

58. Gardner, T., K. Stanish, and M. Alexander. Critical review of rapid chloride test methods for concrete. *Concrete Beton Magazine*, 2006. 113: 11-17.

59. Andrade, C. Calculation of chloride diffusion coefficients in concrete from ionic migration measurements. *Cement and Concrete Research*, 1993. 23 (3): 724-742.

60. Buenfeld, N. R., G. K. Glass, A. M. Hassanein, and J. Z. Zhang. Chloride transport in concrete subjected to electrical field. *Journal of Materials in Civil Engineering (ASCE)*, 1998. 10 (4): 220-228.

61. Lothenbach, B., K. Scrivener, and R. D. Hooton. Supplementary Cementitious Materials. *Cement and Concrete Research*, 2011. 41 (12): 1244-1256.

62. Monfore, G. E. The Electrical Resistivity of Concrete. *Journal of the PCA Research and Development Laboratories*, 1968. 10 (2): 35-48.

63. Pfeifer, D. W., D. B. McDonald, and P. D. Krauss. The Rapid Chloride Permeability Test and Its Correlation to the 90-Day Chloride Ponding Test, 1994. *PCI Journal*, 1994. 39 (1): 38-47.

64. Plauto, P., and A. Bilodeau. Rapid chloride ion permeability test: Data on concretes incorporating supplementary cementing materials. Proc., 3rd Int. Conf. on the Use of Fly Ash, Silica Fume, Slag, and Natural Pozzolan in Concrete, *American Concrete Institute (ACI)*, SP 114, Trondheim, Norway, 1989. 625-644.

65. Mobasher, B., and T. M. Mitchell. Laboratory Experience with the Rapid Chloride Permeability Test. *ACI SP-108*: Permeability of Concrete, (ed. D. Whiting, A. Walitt), American Concrete Institute, 1988.

66. El Dieb, A. S. Evaluating Concrete Durability Using Simple Non–Destructive Test Towards Performance–Based Specification. *MOJ Civil Engineering*, 2018. 4 (2): 100-102.

67. Federal Highway Administration Research and Technology. *Surface Resistivity Test Evaluation as an Indicator of the Chloride Permeability of Concrete*, 2012. FHWA-HRT-13-024.

68. Streicher, P. E., and M. G. Alexander. A Chloride Conduction Test for Concrete. *Cement and Concrete Research*, 1995. 25 (6): 1284-1294.